

2
min
mix

X-630-72-206

PREPRINT

NASA TM X- 66073

THE INTERSTELLAR LINE SPECTRA OF ZETA OPHIUCHI AND ZETA PERSEI AND THEIR RELATION TO THE SHORT WAVELENGTH MICROWAVE BACKGROUND RADIATION

VICTOR JOHN BORTOLOTT, JR.

(NASA-TM-X-66073)	THE INTERSTELLAR LINE SPECTRA OF ZETA OPHIUCHI AND ZETA PERSEI AND THEIR RELATION TO THE SHORT WAVELENGTH MICROWAVE BACKGROUND	V.J. Bortolot, Jr.	N73-11812
(NASA)	Jun. 1972	123 p	CSSL 03B G3/29 46431
			Unclas

JUNE 1972

Goddard Institute for Space Studies
New York, New York



GODDARD SPACE FLIGHT CENTER
GREENBELT, MARYLAND



Reproduced by
**NATIONAL TECHNICAL
INFORMATION SERVICE**
U S Department of Commerce
Springfield VA 22151

123 P.

THE INTERSTELLAR LINE SPECTRA OF
ZETA OPHIUCHI AND ZETA PERSEI
AND THEIR RELATION TO THE SHORT WAVELENGTH
MICROWAVE BACKGROUND RADIATION

Victor John Bortolot, Jr.

A dissertation in the Department of Physics submitted to the faculty
of the Graduate School of Arts and Science in partial fulfillment of
the requirements for the degree of Doctor of Philosophy at New York
University.

1^c

June 1972

ABSTRACT

Thirty-one high dispersion coude spectrograms of ζ Oph ($V = 2.57$, MK-type O9.5V, $b^{\text{II}} = +23^{\circ}$) and seven of ζ Per ($V = 2.83$, MK-type B1Ib, $b^{\text{II}} = -17^{\circ}$) have been numerically synthesized to produce high resolution, low-noise spectra in the interval $\lambda\lambda 3650 - 4350 \text{ \AA}$ that yield more accurate data on atomic and molecular absorption in well-defined regions of the interstellar medium. The detection threshold is improved by as much as a factor 5 over single plates. Several new interstellar lines have been discovered in the ζ Oph -15 km sec^{-1} cloud and the ζ Per $+13 \text{ km sec}^{-1}$ cloud. $\text{C}^{13}\text{H}^+ \lambda 4232 \text{ \AA}$ and KI $\lambda\lambda 4043$ and 4047 \AA are seen in ζ Oph for the first time anywhere in the interstellar medium, and the previously observed Ca I $\lambda 4227 \text{ \AA}$ and Fe I $\lambda\lambda 3720$ and 3860 \AA for the first time in both ζ Oph and ζ Per. Their equivalent widths range from 0.3 to 2 m \AA . Ca I $\lambda 4227 \text{ \AA}$, with the strong Ca II H and K interstellar lines, yields the ionization equilibrium and hence the electron density. Reasonable limits on the photoionization rate computed from recently proposed galactic and stellar radiation fields yield $n_e = 0.16 - 0.55 \text{ cm}^{-3}$ in the ζ Oph -15 km sec^{-1} cloud and $n_e = 0.044 - 0.14 \text{ cm}^{-3}$ in the ζ Per $+13 \text{ km sec}^{-1}$ cloud.

The neutral hydrogen density is estimated to be $50 - 700 \text{ cm}^{-3}$ in the ζ Oph cloud and $10 - 80 \text{ cm}^{-3}$ in ζ Per for reasonable assumptions of the cosmic ray ionization rate of hydrogen and the abundance of easily ionized trace elements. Sodium and potassium appear in the ζ Oph cloud approximately at their solar system abundances relative to hydrogen, but calcium, iron, and aluminum seem to be deficient by large factors — 2500, 300, and > 100 , respectively. The abundances in ζ Per relative to sodium are similar, suggesting that most of the iron, aluminum, and perhaps other metals is bound up in the interstellar grains.

$\text{C}^{13}\text{H}^+ \lambda 4232 \text{ \AA}$ in ζ Oph yields a $[\text{C}^{12}]/[\text{C}^{13}]$ ratio of 81 (+ 113, -16), consistent with terrestrial value 89. This suggests that C^{13} -rich stars have not contributed much to the interstellar medium, at least in the vicinity of the sun, and that its composition has not changed much in the past 5×10^9 years.

The CN, CH, and CH^+ bands at $\lambda\lambda 3875, 4300, \text{ and } 4232 \text{ \AA}$ provide in all one precise measurement of the microwave background radiation brightness temperature and three upper limits at millimeter and submillimeter wavelengths. The CN excitation temperatures, corrected for local processes, yield $T_B(\lambda 2.64 \text{ mm}) = 2.75 \pm 0.10^\circ \text{ K}$ in ζ Oph and $2.66 \pm 0.12^\circ \text{ K}$ in ζ Per. The upper

limits on the background radiation intensity in units of $\text{erg cm}^{-2} \text{sec}^{-1} \text{ster}^{-1} \text{Hz}^{-1}$ are 0.72×10^{-14} at 1.32 mm (CN), 1.66×10^{-14} at 0.56 mm (CH) and 3.75×10^{-14} at 0.36 mm (CH^+). The CN excitation in six stars, including late B and early A giants, is found to be consistent with 2.8°K and consistent with a universal CN excitation mechanism.

ACKNOWLEDGEMENTS

I am first of all grateful to my dissertation advisor Patrick Thaddeus for a first rate and demanding education in physics and astronomy. I would like to thank the Director of the Lick Observatory for an exceptionally generous grant of observing time, and the Director of the Goddard Institute for Space Studies for his hospitality. I am grateful to NASA and the NYU Physics Department for my financial support. Thanks are due to Seth Shulman for his considerable and cheerful help in digitizing the spectrograms and for many valuable discussions, to E. L. Schucking and R. E. White for their advice and encouragement, to R. Kocornick and N. Kastan for their help in programming, to T. Psaropulos for his fine draftsmanship, and to everybody in technical typing at Goddard, who saw this dissertation through countless drafts to the final version.

I could not have done this without the constant support and encouragement of my wife, Jeanne, who is still my best friend.

TABLE OF CONTENTS

		Page
I.	INTRODUCTION	1
II.	THE -15 KM SEC^{-1} CLOUD IN ζ OPHIUCHI	5
	a) Spectrograms	7
	b) Results of Plate Analysis	8
	c) Electron Density and Atomic Abundances	12
	i) Ionization Equilibrium	13
	ii) The Radiation Field	14
	iii) Atomic Photoionization Cross-Sections and Recombination Rates	16
	iv) The Electron Density	17
	v) Atomic Abundances	18
	vi) The Hydrogen Density and the Degree of Ionization	20
	vii) Metastable Helium and the Cosmic Ray Ionization Rate	25
	d) Interstellar $\text{C}^{13} \text{H}^+$	26
III.	The $+13 \text{ KM SEC}^{-1}$ CLOUD IN ζ PERSEI	33
	a) Observational Results	33
	b) The Electron Density and the Atomic Abundances	36

IV.	THE SPECTRUM OF THE MICROWAVE BACKGROUND RADIATION	39
	a) The Molecular Excitation Temperatures	41
	b) CN Excitation by Local Processes	46
	i) Neutral Particle Collisions	49
	ii) Electron Impact	49
	iii) Proton Impact	50
	iv) Optical Photoexcitation	51
	c) Discussion of the Short Wavelength Observations	52
	d) Invariance of the CN Excitation	54
	i) Observational Results	55
	ii) Discussion	58
V.	SUMMARY AND CONCLUSIONS	61
	APPENDICES	
	A. Densitometry	64
	B. Statistical Analysis of Upper Limits	68
	C. Statistical Errors in Equivalent Width Measurements	73

I. INTRODUCTION

Soon after the discovery of the microwave background radiation by Penzias and Wilson (1965), it was recognized that the optical absorption lines of the interstellar molecules CN, CH, and CH^+ might be used to determine the radiation brightness temperature at certain millimeter and submillimeter wavelengths (Field and Hitchcock 1966; Thaddeus and Clauser 1966). The background photons at the wavelengths of molecular resonances will rotationally excite the molecules in interstellar space, and hence will be detectable optically by the presence of band spectra. The relative intensities of absorption lines which arise from different lower levels will yield the brightness temperature of the background radiation at the transition wavelength connecting those levels.

It had long been known that the first excited rotational level of CN, whose $J = 0 \rightarrow 1$ transition resonance falls at λ 2.6mm, was populated in interstellar space. On the basis of visual estimates by Adams (1941) of the intensities of the R(0) and R(1) lines of the interstellar (0,0) violet band in the bright O star ζ Oph, McKellar (1941) computed the excitation temperature of this level to be 2.3° K. Hardly any significance was attached to this result at the time, it presumably being thought that the excitation was due to "local" interstellar processes.

The first modern use of CN as a thermometer at the λ 2.6mm resonance yielded excitation temperatures against ζ Oph and ζ Per that agreed both with the Penzias and Wilson (1965) λ 7.35cm radio measurement and with each other (Field and Hitchcock 1966; Thaddeus and Clauser 1966). The agreement between the two molecular excitation temperatures suggested that the effect of local interstellar excitation mechanisms was small and that the excitation temperatures were actually quite close to the brightness temperature.

Interstellar lines observed optically are never strong, and those of CN in particular are found only in a handful of stars. The technique of plate synthesis, where a number of spectrograms of a star are added together, may be used to improve the signal-to-noise ratio of the weak molecular bands. The first application of this technique to background radiation measurements made use of existing plates, many obtained by Adams and Dunham in the 1930's and 40's (Clauser 1970; Clauser and Thaddeus 1972). In addition to more accurate λ 2.6mm CN temperatures in ζ Oph and ζ Per, this work established upper limits at three shorter wavelengths - $\lambda\lambda$ 1.32, 0.56, and 0.36 mm of CN, CH, and CH^+ , respectively. Data from a number of other stars were cited as evidence for the directional invariance of the CN excitation.

This dissertation began as an attempt to still further improve the observational data on CN, CH, and CH^+ by the acquisition of new observations. About fifty high resolution plates were obtained at the Lick Observatory 120-inch telescope coude spectrograph, including 31 of the most favorable star, ζ Oph, and 7 of ζ Per, where the CN lines (but not those of CH or CH^+) are about as strong as in ζ Oph. Preliminary results of the ζ Oph plate synthesis have been reported (Bortolot, Clauser, and Thaddeus 1969). In this dissertation, a significant improvement over those findings will be presented, along with new data on ζ Per and other stars which pertain to the question of directional invariance.

A good part of this dissertation will treat the syntheses, covering the entire interval $\lambda\lambda 3650$ to 4350 \AA , of ζ Oph and ζ Per, both stars exceptionally rich in interstellar molecular and atomic absorption in spite of their relative closeness to the sun and moderate reddening. Although previous work on the synthesis technique involved only narrow intervals about strong absorption features (e.g. Augason and Herbig 1967; Bortolot et al. 1969), much effort was expended in the present work to synthesize entire plates, to take advantage of the considerable information on the interstellar medium they contain.

The great increase in sensitivity of the syntheses over single plates (more than five-fold for ζ Oph) permits more accurate data to be obtained on interstellar atomic and molecular abundances than previously possible. These abundances in turn will form the basis of more accurate calculations of the ionization equilibrium and molecular processes.

The interstellar line profiles in the spectra of the two stars we consider here are reasonably simple — that is, resolvable into distinct clouds with little overlap. We thus avoid the problem of interpretation occurring in studies of distant stars where the lines are formed in multiple overlapping clouds. The analysis of such lines must lead to some sort of average physical conditions which conceivably might not apply to the average cloud.

In the next section we will deal with the ζ Oph observations, first obtaining the atomic and molecular column densities, then deriving from them the ionization equilibrium, and finally deducing the abundances. Of considerable interest will be the upper limits on undetected lines. The third section, on ζ Per, will present essentially this same analysis on a different cloud. The measurements of the background radiation and a discussion of the molecular excitation mechanisms in the ζ Oph cloud will comprise the fourth section.

II. THE -15 km sec^{-1} CLOUD IN ζ OPHIUCHI

The interstellar line spectrum of ζ Oph ($V = 2.57$, MK-type O9.5V, $b^{\text{II}} = +23^\circ$) has probably been more thoroughly studied than that of any other star. Adams (1949) noted there the presence of every then-known interstellar line with the exception of those of Fe I and Ca I. The optical lines in ζ Oph appear to be resolvable into distinct clouds which hardly overlap. At conventional dispersions, they are double, the strongest component lying at -15 km sec^{-1} and a weaker one at -29 km sec^{-1} . The high resolution Fabry-Perot observations of Hobbs (1965) have indicated structure at the bottom of the strong -15 km sec^{-1} line and at least four other components, near -9 , -26 , -28 , and -33 km sec^{-1} .

Herbig (1968) has given a quite thorough discussion of the physical conditions and the atomic and molecular abundances in the -15 km sec^{-1} cloud, and it would be worthwhile to briefly summarize his results. A curve of growth analysis has yielded doppler constants for Na I, Ca II, and CH^+ , and the column densities of Na I, Ca II, K I, CN, and CH. Although there is an extensive H II region surrounding ζ Oph, roughly 15 pc in radius, it is argued that the -15 km sec^{-1} cloud is wholly an

H I region on the grounds that (1) the pattern of the optical absorption lines is consistent over an area of the sky considerably larger than that covered by the ionized region; (2) the 21-cm line velocities show general agreement with this pattern; (3) if the Na I lines were formed in the H II region, the Na/H abundance ratio would be inconsistent with the solar system value; and (4) the rms turbulent velocities observed in H II regions are an order of magnitude greater than those determined from the curve of growth analysis in the -15 km sec^{-1} cloud. As the H II region is expected to be at least roughly spherical in shape, Herbig placed the cloud at a minimum distance of 15 pc from ζ Oph. On the assumption that ζ Oph dominates the radiation field and that there is no attenuation by the cloud, he computed the electron density in ionization equilibrium (see Equation (1), below) at a point 20 pc from the star. From an upper limit on the Ca I/Ca II line ratio, he obtained $n_e < 1.9 \text{ cm}^{-3}$, but on the assumption that the Na/H abundance ratio had the solar system value 2.4×10^{-6} , he deduced the ratio Na I/Na II and found $n_e = 0.35 \text{ cm}^{-3}$. With this electron density and the assumed radiation field, potassium was found to be normally abundant relative to sodium, while calcium was deficient by more than three orders of magnitude and titanium by at least two. He also deduced that the cloud was

possibly a thin (0.15 pc) sheet with the rather high neutral hydrogen density $500 - 900 \text{ cm}^{-3}$.

In this chapter we will apply the plate synthesis technique to improve Herbig's observational data in the spectral region $\lambda\lambda 3650 - 4350 \text{ \AA}$, and to search for new interstellar lines. We then will discuss the physical conditions and abundances in the cloud, taking advantage of recent observational and theoretical work not available to Herbig, particularly in the discussion of the radiation field and the neutral hydrogen density.

a) Spectrograms

A total of 31 spectrograms of ζ Oph in the region $\lambda\lambda 3650 - 4350 \text{ \AA}$ were obtained with the coude spectrograph of the Lick Observatory 120-inch telescope in 1968-9. The dispersion with the 160-inch camera was 1.3 \AA mm^{-1} and the resolving power $\lambda/\Delta\lambda$ was 85 000. The spectrograms were 20 inches long, consisting of two 10-inch plates exposed end-to-end in the spectrograph plate holder. The emulsion was Eastman Kodak Ila-O, baked at 50° C for 60 hours, and developed in D-76 for 15 minutes. The projected slit width was 35 microns and the spectra

were quite wide — about 5 mm, in order to store a good deal of information on each plate. The average exposure time was 45 minutes.

Densitometry was carried out on the D. W. Mann model 1140 microdensitometer at the Goddard Institute for Space Studies. The output from the photomultiplier of the densitometer was digitized and, together with the comparator screw position, was recorded on magnetic tape every 4 microns of plate travel. Subsequent processing of the spectrograms was entirely digital. The methods of wavelength and intensity calibration and digital spectrum synthesis are described in Appendix A. The equivalent widths were measured numerically: an intensity continuum was first fit to the vicinity of the line; the spectrum was then normalized to this continuum; finally, a numerical integration over the line gave the equivalent width. The procedure for numerical determination of upper limits is discussed in Appendix B.

b) Results of Plate Analysis

An example of the marked increase in sensitivity provided by the plate synthesis of ζ Oph is shown in Figure 1. The Fe I line at $\lambda 3860 \text{ \AA}$ shown in this figure cannot be seen on a single

good plate, is barely detectable in a synthesis of six plates, but is unmistakable when all 31 plates are synthesized. The equivalent width of this line is only $1 \text{ m}\text{\AA}$, or about one-half that of the faintest lines discernable on a single high quality plate.

The atomic and molecular lines detected in the range $\lambda\lambda 3650 - 4350 \text{ \AA}$ are shown in Figures 2 and 3. Table 1 lists the measured equivalent widths and radial velocities, and upper limits to the equivalent widths of the most important lines not detected. Herbig's (1968) data are also included for the sake of comparison.

Three lines, K I $\lambda 4044 \text{ \AA}$, $\lambda 4047 \text{ \AA}$, and $\text{C}^{13}\text{H}^+ \lambda 4232 \text{ \AA}$, are detected in the interstellar medium for the first time. Three others, Ca I $\lambda 4227 \text{ \AA}$ and Fe I $\lambda 3720 \text{ \AA}$ and $\lambda 3860 \text{ \AA}$ are new in ζ Oph. These lines, as Figures 2 and 3 show, fall at -15 km sec^{-1} , the velocity of the strong atomic and molecular lines. The Ca I line, which with H or K of Ca II allows determination of the ionization equilibrium, has been seen previously against χ^2 Ori and several other stars. A preliminary analysis of the C^{13}H^+ line has been given (Bortolot and Thaddeus 1969).

A number of interstellar lines were sought but not found. A search for all the resonance lines of the elements tabulated in

the Charlotte Moore Tables (1945) falling in the interval $\lambda\lambda 3650 - 4350 \text{ \AA}$ yielded upper limits of 0.5 m\AA or less, with the upper limit corresponding to a confidence level of 99 percent. Accordingly, 0.5 m\AA may be taken as a general upper limit for any missing line. Some upper limits of particular importance are included in Table 1, and will be discussed in later sections.

In order to determine the optical depths and column densities of the atoms and molecules observed, some assumption concerning the curve of growth is necessary. By fitting the equivalent widths of the Na I and CH^+ lines to a curve of growth for a gaussian velocity distribution, Herbig (1968) obtained the doppler constants $b(\text{Na I}) = 2.43 \text{ km sec}^{-1}$ and $b(\text{CH}^+) = 0.85 \text{ km sec}^{-1}$. Uncertainties in the CH^+ Franck-Condon factors make the latter value somewhat doubtful. Hegyi, Traub, and Carleton (1972, to be published) have recently resolved the CN R(0) line in ζ Oph with a Fabry-Perot spectrometer. When their linewidth is corrected for instrumental broadening and line saturation, $b(\text{CN})$ is found to be 1.36 km sec^{-1} . This doppler constant, if caused by thermal line broadening, would indicate a kinetic temperature in excess of 1000° K — far above that of normal H I regions — and hence the line broadening is probably caused by microturbulence. On the assumption that the CN, CH, and CH^+ molecules which are observed are well mixed

together, it will be assumed that $b = 1.36 \text{ km sec}^{-1}$ applies to all the molecular lines. Fabry-Perot work in progress by Hobbs (1972, private communication) on $\text{CH}^+ \lambda 4232 \text{ \AA}$ will provide a check of this value. The doublet ratio method of Strömberg (1948) is well suited for determination of $b(\text{Ca II})$ from the moderately strong H and K lines and yields $b(\text{Ca II}) = 1.92 \text{ km sec}^{-1}$. The Ca II column density and those of the molecules, determined with the doppler constants just discussed, are given in Tables 2 and 3; the column densities in these tables corresponding to the weak, presumably unsaturated, lines are taken from the linear part of the curve of growth which is independent of doppler constant.

The CN, CH, and CH^+ lines near $\lambda\lambda 3875, 4300, \text{ and } 4232 \text{ \AA}$ used for determination of the microwave background temperature are shown in Figures 4, 5, and 6; Table 4 contains the equivalent widths and corresponding optical depths of these lines. Upper limits on the equivalent widths of those lines not observed were calculated according to the procedure of Appendix B. For these lines, the intensity continuum was taken to be the best straight line fit to a 1 to 2 \AA interval about the expected wavelength; this is shown superimposed on the lowest spectrum in Figures 4 through 6.

It is well known that systematic differences of the order of 25 percent exist in equivalent width measurements at different

observatories (see, e. g., Wright 1969, Frisch 1972), but for determination of excitation conditions and the microwave background temperature only the ratio of line intensities is important. With respect to relative intensities, it is estimated that the errors in intensity calibration (see Appendix A) are negligible in comparison to the statistical uncertainties of equivalent width measurement, at least for faint lines. Statistical uncertainties are discussed in Appendix C, and are given for the CN lines in Table 12.

Table 1 shows that no systematic difference in radial velocity exists between various atomic and molecular lines. This obviously supports the idea that the -15 km sec^{-1} cloud is rather homogeneous, and that the atoms and molecules are all well mixed. A possible exception to this is found in $\text{CH}^+ \lambda 3958 \text{ \AA}$, which is about 0.01 \AA to the blue of its expected wavelength. Herbig seems to observe the same effect, and it appears also in the ζ Per observations to be discussed. The most likely explanation is that the rest wavelength of Douglas and Herzberg (1942), which was not directly measured but was computed from the molecular constants derived from other bands, is somewhat in error.

c) Electron Density and Atomic Abundances

We turn now to the problem of extracting from the column densities as much information as possible on the physical conditions and abundances within the -15 km sec^{-1} cloud.

i) Ionization Equilibrium

The detection of Ca I $\lambda 4227 \text{ \AA}$ in the -15 km sec^{-1} cloud permits there for the first time a direct evaluation of the ionization equilibrium and the electron density. In ionization equilibrium (see, e.g., Spitzer 1968),

$$\frac{n(X_{r+1}) n_e}{n(X_r)} = \frac{\Gamma_r}{\alpha_r} \quad (1)$$

where $n(X_r)$ is the number density of the element X in the r^{th} stage of ionization, n_e is the electron density, Γ_r is the photoionization rate, and α_r is the total recombination rate to the r^{th} stage of ionization. The photoionization rate is given by

$$\Gamma = h^{-1} \int_0^{\infty} a_{\lambda} u_{\lambda} \lambda d\lambda \text{ sec}^{-1} \quad (2)$$

where a_{λ} is the photoionization cross section, u_{λ} is the radiation density, and h is Planck's constant (we have dropped the subscript r in Equation (2) since we are dealing only with neutral and singly ionized atoms). Thus, the observed Ca II/Ca I density ratio permits computation of n_e as a function of the radiation field; in turn, the electron density allows one to compute abundances of the elements observed, provided that their photoionization cross sections and recombination rates are known for all accessible stages of ionization. The only dependence of Equation (1) on the kinetic temperature is

~~recombination rates are known for all accessible stages of ionization.~~

~~The only dependence of Equation (1) on the kinetic temperature is~~
through $\alpha \sim T^{-0.4}$. Estimates of T_{kin} range from 50 - 125° K and 100° K is adopted. The resulting uncertainty in the ionization equilibrium is only about 25 percent - at most comparable to that of other quantities in the equation - and will be neglected.

ii) The Radiation Field

The radiation field of optical photons in the -15 km sec^{-1} cloud is presumably the general galactic field plus that of ζ Oph, attenuated by the cloud itself. Instead of the galactic spectrum computed by Zimmermann (1964) which Herbig used in his analysis, we will adopt the field recently calculated by Habing (1968) on the basis of new measurements of the interstellar extinction and the ultraviolet flux from OB stars. Using rocket, satellite, and ground-based data to separate the airglow and zodiacal light contributions to the sky brightness, Lillie (1968) has found a radiation density of $35 - 55 \times 10^{-18} \text{ erg cm}^{-3} \text{ \AA}^{-1}$ at $\lambda 2000 \text{ \AA}$, in good agreement with Habing's values $30 \times 10^{-18} \text{ erg cm}^{-3} \text{ \AA}^{-1}$ at $\lambda 2200 \text{ \AA}$ and $50 \times 10^{-18} \text{ erg cm}^{-3} \text{ \AA}^{-1}$ at $\lambda 1400 \text{ \AA}$. For the stellar field we will adopt, as did Herbig, the radiative flux from the B0V line-blanketed stellar-atmosphere model of Hickok and Morton (1968), taking the stellar radius to be $8 R_{\odot}$. It will also be assumed, following Herbig, that the -15 km sec^{-1} cloud is an H I region which is at least 15 pc from ζ Oph, thereby setting an upper limit to the contribution of ζ Oph to the total radiation field.

Consider now the attenuation of these fields by the cloud. The color excess of ζ Oph has been determined by Bless and Savage (1970) to be $E_{B-V} = +0.28$, which according to Whitford (1958) represents a total extinction of 0.87 mag at $\lambda 5480 \text{ \AA}$. It is reasonable to assume that this extinction is produced mainly by the -15 km sec^{-1} cloud, and that the extinction at the center of the cloud is 0.44 mag. The ζ Oph reddening curve has a hump at $\lambda 2200 \text{ \AA}$ and increases with inverse wavelength somewhat faster than the customary λ^{-1} law. If the grains within the cloud have appreciable albedo, however, scattered starlight will reduce the attenuation in the cloud markedly from that expected if the extinction were purely absorptive. Habing (1968) gives a simple approximate expression for the attenuation factor G as a function of albedo a and the total extinction $A(\lambda)$ in a homogeneous cloud, namely

$$G = \left[a + (1-a)10^{0.4A(\lambda)} \right]^{-1} \quad (3)$$

New observations of the general galactic field by Witt and Lillie (1971) indicate that the albedo has a minimum of 10 percent at the position of the extinction hump ($\lambda 2200 \text{ \AA}$) and rises sharply to 90 percent at $\lambda 1500 \text{ \AA}$. In the short wavelength region, then, where the albedo is near unity there is not much absorption of photons even though the total extinction may exceed 3 magnitudes.

Since the actual position of the -15 km sec^{-1} cloud is poorly known, we are led to adopt two cases which hopefully bracket the range of possible

radiation densities: (1) a "high" field which is the sum of the galactic and the stellar radiation at 15 pc from ζ Oph, attenuated by the factor G computed from the reddening curve of Bless and Savage and the albedo data of Witt and Lillie; and (2) a "low" field which is the attenuated galactic radiation alone. These "high" and "low" fields as a function of wavelength are shown in Figure 7.

iii) Atomic Photoionization Cross-Sections
and Recombination Rates

For Ca I we follow Herbig in piecing together the photoionization cross-sections at different wavelengths of Hudson and Carter (1967a), Newsom (1966), and Ditchburn and Hudson (1960): the composite is shown in Figure 8. For Na I and K I, we use the cross-sections of Hudson and Carter (1967b and 1965). For the Al I cross-section we adopt the experimental data of Kozlov, Nikonova, and Startsev (1966) in the region $\lambda\lambda 1550 - 2070 \text{ \AA}$, and the calculation of Burgess, Field, and Michie (1960) at shorter wavelengths. For Fe I, we use the recent theoretical cross-section of Kelly and Ron (1971), based on many-body perturbation theory, which is considerably larger than the Hartree-Fock value in the region $\lambda 912 - 1970 \text{ \AA}$.

The recombination rates of Ca I, Na I, and K I are taken from Seaton (1951) and that of Al I from Burgess, Field, and Michie (1960).

The recombination rate of Fe I is highly uncertain; a value $0.6 \times 10^{-11} \text{ sec}^{-1}$, comparable to that of the other atoms, will be adopted.

Table 4 lists the atomic photoionization rates computed from Equation (2) for the two adopted radiation fields and the adopted recombination rates.

iv) The Electron Density

In order to calculate the electron density with Equation (1) we make the additional assumption that low density matter at $\sim 15 \text{ km sec}^{-1}$ exterior to the cloud does not contribute to the observed equivalent widths of the calcium lines, an effect which Herbig estimates will influence the column densities by less than a factor 2. Equation (1) then yields with the Ca I / Ca II line ratio and the appropriate Γ/α an electron density equal to 0.55 cm^{-3} for the high field and 0.16 cm^{-3} for the low. If the albedo data were grossly in error, the electron density could be as high as 0.75 cm^{-3} - corresponding to a completely unattenuated high field - or as low as 0.07 cm^{-3} - an attenuated low field where there is no scattered galactic light. We consider neither of these cases likely. In his calculation of the electron density, Herbig (1968) assumed essentially the unattenuated high field at a star-cloud distance of 20 pc. Using the assumed normal abundance of sodium

relative to hydrogen to estimate $N(\text{Na II})$, he obtained the electron density $n_e = 0.35 \text{ cm}^{-3}$.

The total column density of sodium may now be determined without Herbig's assumption that the Na/H ratio has the solar system value. Taking the column density he determined from the observed D and D' lines, $N(\text{Na I}) = 5 \times 10^{13} \text{ cm}^{-2}$, Equation (1) yields for the total sodium column density $N(\text{Na}) = 6.1 \times 10^{14} \text{ cm}^{-2}$. For the hydrogen column density Stecher (1968) finds $N(\text{H I}) = 4.2 \times 10^{20} \text{ cm}^{-2}$ from rocket measurement of Lyman α . The Na/H abundance ratio is then found to be 1.5×10^{-6} , which is indeed consistent with the solar system value 2.4×10^{-6} (Cameron 1968).

It should be remarked that $N(\text{Na})$ is insensitive to the adopted radiation field. On substituting $n_e = \Gamma_{\text{Ca}} N(\text{Ca I}) / \alpha_{\text{Ca}} N(\text{Ca II})$ into the sodium ionization equation it becomes apparent that the only dependence of $N(\text{Na})$ on the radiation field is through the ratio $\Gamma_{\text{Na}} / \Gamma_{\text{Ca}}$. As may be seen from Table 5, this ratio and also the ratios K/Ca, Fe/Ca, and Al/Ca are insensitive to the exact radiation field.

v) Atomic Abundances

Table 5 lists the atomic abundances computed from Equation (1) and the data in Tables 2 and 4. The values quoted are an average

of those found for the high and low fields which differ typically by less than 20 percent. Sodium and potassium relative to hydrogen have their normal solar system abundances, within the observational uncertainties. Gaseous calcium here, as elsewhere (cf. Howard, Wentzel, and McGee 1963), seems to be deficient by a large factor. The factor 2500 here is, however, somewhat greater than generally observed.

Iron and aluminum also appear to be deficient by large factors in the gas phase. From the Fe I column density, $N(\text{Fe I}) = 3.5 \times 10^{11} \text{ cm}^{-2}$, and the data in Table 4, the total iron column density is found to be $4.3 \times 10^{13} \text{ cm}^{-2}$. The Fe/H ratio is then 1.0×10^{-7} , almost three orders of magnitude below the solar system value. This discrepancy is probably not attributable to uncertainty in the calculation of the photoionization cross-section (Kelly 1971, private communication). One cannot evaluate precisely the uncertainty in the recombination rate, but it is presumably less than an order of magnitude.

An important result of the observations is the apparently large underabundance of aluminum in the -15 km sec^{-1} cloud. The $0.26 \text{ m}\text{\AA}$ upper limit for Al I $\lambda 3944 \text{ \AA}$ yields $N(\text{Al I}) < 6 \times 10^{10} \text{ cm}^{-2}$. We obtain an upper limit on the total column density of aluminum

$N(\text{Al}) < 1.1 \times 10^{13} \text{ cm}^{-2}$, which then gives an Al/H ratio of less than 2.6×10^{-8} , a factor of at least 100 less than the fractional abundance in the solar system (Cameron 1968).

It is unlikely that new atomic data will remove the large deficiencies of iron and aluminum, and our results consequently support the idea that most of these metals is trapped in the interstellar grains. Herbig (1968) has noted also a titanium underabundance in the -15 km sec^{-1} cloud by a factor greater than 100. The question of deficient calcium has not been satisfactorily answered. For the radiation fields adopted, the ionization of Ca II should be negligible and other depletion mechanisms must be considered. Goldsmith, Field, and Habing (1969) have attempted to explain the low abundance of calcium relative to sodium by differences in their rates of accretion on grains, but found that the differences are not sufficient to produce the required Ca/Na ratio without seriously depleting both these elements relative to hydrogen.

vi) The Hydrogen Density and the Degree of Ionization

It is possible to estimate the neutral hydrogen density from the electron density if we assume normal cosmic abundances of the predominantly once-ionized elements carbon, magnesium, silicon, and iron. Charge neutrality gives

$$n_e = n(\text{H II}) + n(\text{C II}) + n(\text{Mg II}) + n(\text{Si II}) + n(\text{Fe II}) \quad ; \quad (4)$$

the right-hand side of which may be written $n(\text{H II}) + \epsilon n(\text{H I})$, where $\epsilon = 6 \times 10^{-4}$ according to the abundances given by Cameron (1968).

The ionization equilibrium for hydrogen is

$$\frac{n(\text{H II})n_e}{n(\text{H I})} = \frac{\zeta}{\alpha} \quad , \quad (5)$$

where ζ is the total cosmic ray and soft X-ray ionization rate and α is the total recombination rate to all but the ground state. (Since the cloud is assumed to be an H I region, there is no photoionization of hydrogen.) According to Seaton (1959), $\alpha = 0.69 \times 10^{-11} \text{sec}^{-1}$.

Therefore we arrive at an expression for n_e in terms of $n(\text{H I})$ and ζ ,

$$n_e = \frac{\epsilon n(\text{H I})}{2} + \frac{1}{2} \left[\epsilon^2 n(\text{H I})^2 + 4\zeta n(\text{H I})/\alpha \right]^{1/2} \quad . \quad (6)$$

The energetic particle ionization rate ζ is highly uncertain. Spitzer and Tomasko (1968) give the upper and lower limits $1.17 \times 10^{-15} \text{sec}^{-1}$ and $6.8 \times 10^{-18} \text{sec}^{-1}$ for ionization due to cosmic rays, and a recent calculation by Hjellming, Gordon, and Gordon (1969), based on dispersion of pulsar signals, indicates that $\zeta \approx 2.5 \times 10^{-15} \text{sec}^{-1}$. Silk and Werner (1968) estimate that the

ionization rate due to X-rays which have passed entirely through the hydrogen in the galactic plane is about $8 \times 10^{-17} \text{ sec}^{-1}$ — probably small with respect to that of cosmic rays.

A further uncertainty that must be considered is the possible depletion of the easily ionizable elements, notably carbon, by accretion on grains. A set of depletion factors has been computed by Goldsmith, Habing, and Field (1969): they find the factors 2, 10, 5, and 3 for O I, C II, Si II, and Fe I, respectively, at an accretion time of 7×10^7 years. (The ions accrete more rapidly since collisions with fast moving electrons produce a negative charge on the grains.) We will assume that the Mg II is depleted by the same factor as Si II. The deficiencies of iron and aluminum noted in the preceding section are highly suggestive of this depletion. Smith (1972, to be published) has obtained a rocket UV spectrum of ζ Oph which indicates that carbon is depleted by a factor no more than five. Thus the depletion factors of Goldsmith et al. (1969) for the major trace elements lead to a reasonable lower limit on their abundance with respect to hydrogen.

These lowered abundances lead to $\epsilon = 0.7 \times 10^{-4}$. Although the effect of this decrease on n_e is quite large when ζ is small, it is minimal up to rather high values of $n(\text{H I})$ when $\zeta = 1.17 \times 10^{-15} \text{ sec}^{-1}$. Figure 9 shows n_e versus $n(\text{H I})$ for the two values of ϵ and several values of ζ . We distinguish two cases:

1. Normal ϵ . The effect of cosmic ray ionization is small for $n(\text{H I}) > 300 \text{ cm}^{-3}$; for $n(\text{H I}) = 10 \text{ cm}^{-3}$, cosmic rays produce nearly a factor 10 more electrons than the easily ionizable elements. Given the limits $n_e = 0.16$ to 0.55 cm^{-3} , $n(\text{H I})$ falls in the range $260 - 900 \text{ cm}^{-3}$ for $\zeta = 0$, $90 - 570 \text{ cm}^{-3}$ for $\zeta = 1.17 \times 10^{-15} \text{ sec}^{-1}$, and $50 - 440 \text{ cm}^{-3}$ for $\zeta = 2.5 \times 10^{-15} \text{ sec}^{-1}$.

2. Depleted ϵ . The effects of cosmic ray ionization are qualitatively the same. For $\zeta = 0$, $n(\text{H I})$ lies between 2200 and 7900 cm^{-3} ; for $\zeta = 1.17 \times 10^{-15} \text{ sec}^{-1}$, between 130 and 1500 cm^{-3} ; and for $\zeta = 2.5 \times 10^{-15} \text{ sec}^{-1}$, between 60 and 740 cm^{-3} .

One objection to a large hydrogen density is the resulting thinness of the cloud. For a density of 1000 cm^{-3} , the thickness is computed from the hydrogen column density to be about 0.15 pc. This is to be contrasted with the fact that the 15 km sec^{-1} cloud extends over tens of parsecs perpendicular to the line of sight. As Habing (1969) has pointed out, a rough estimate of the lifetime of such a thin cloud based on the observed turbulent velocity (that determined from the curve of growth doppler constant) yields a value comparable to the time needed to establish ionization equilibrium. Thus, for such a thin cloud there is the possibility that any estimate of abundances based on the assumption of ionization equilibrium may be in error.

A more satisfying argument for a low value of $n(\text{H I})$ than the preceding may be derived from an investigation of the energy balance between the cosmic ray heating and the cooling rates in the cloud. Two different models for interstellar H I regions based on this approach have recently been proposed (Field, Goldsmith, and Habing 1969 [FGH]; Hjellming, Gordon, and Gordon 1969 [HGG]). FGH compute the neutral particle density as a function of temperature and trace element depletion for $\zeta = 0.6 \times 10^{-15} \text{ sec}^{-1}$. At 100° K they find $n(\text{H I})$ to be 0.7, 9, and 32 cm^{-3} , for carbon depletion by factors of 1 (normal abundance), 10, and 100, respectively. HGG introduce the hydrogen ionization equation in such a way that the ratios $n_e/n(\text{H I})$ and $\zeta/n(\text{H I})$ can be calculated separately as functions of temperature alone. For 100° K their model predicts $n_e/n(\text{H I}) = 0.01$ and $\zeta/n(\text{H I}) = 0.9 \times 10^{-15} \text{ sec}^{-1} \text{ cm}^{-3}$, leading in the -15 km sec^{-1} cloud to $n(\text{H I})$ between 16 and 55 cm^{-3} and to ζ in the rather high range 14 to $50 \times 10^{-5} \text{ sec}^{-1}$. The HGG model seems to some degree inconsistent with the fairly high electron density found in this cloud; this inconsistency grows worse as the coolants, particularly carbon, are depleted. Since it is not yet possible to decide between the two models by observations (Hobbs and Zuckermann 1972), we will, for the purpose of finding an upper limit to the neutral hydrogen density,

adopt the HGG results and assume that they scale with carbon depletion in the same manner as those of FGH. This gives an upper limit $N(\text{H I}) = 700 \text{ cm}^{-3}$. If the FGH model should prove the more correct, then the limit will be considerably less — below 100 cm^{-3} , even at a kinetic temperature of 30° K .

Taking the lower limit on $n(\text{H I})$ to be about 50 cm^{-3} from the discussion of the hydrogen ionization and the upper limit discussed above, we finally conclude that $n(\text{H I})$ probably falls in the range $50 - 700 \text{ cm}^{-3}$.

vii) Metastable Helium and the Cosmic Ray Ionization Rate

It has been pointed out recently that there may be sufficient interstellar helium in the 2^3S metastable state to cause detectable absorption at $\lambda 3889 \text{ \AA}$ (Scherb 1968, Rees, Sciama, and Stobbs 1968). This state would be populated by recombination to triplet levels following ionization of helium by cosmic rays. According to Rees *et al.* (1968), the life time of the 2^3S state is $2.5 \times 10^8 / [1 + 2.8 \times 10^{-3} y n(\text{H I})]$ sec where the yet unmeasured helium excitation cross-section is given by y ($y \leq 5$) in units of 10^{-16} cm^{-2} . One thus expects the fraction $1.8 \times 10^8 \zeta_{\text{He}} / [1 + 2.8 \times 10^{-3} y n(\text{H I})]$ of the helium atoms to exist in the metastable state. Hence an observation of the $\lambda 3889 \text{ \AA}$ line which arises from this state will set limits on ζ_{He} , which is approximately twice the cosmic ray ionization rate of hydrogen. Our upper limit on $\lambda 3889 \text{ \AA}$, 0.25 m\AA (Table 1), indicates a column density $N(\text{He I}^*) \leq 3 \times 10^{10} \text{ cm}^{-2}$.

If helium is normally abundant, then $N(\text{He I}) = 0.1 N(\text{H I}) = 4 \times 10^{19} \text{ cm}^{-2}$, or $N(\text{He I}^*)/N(\text{He I}) \leq 7 \times 10^{-10}$ and

$$\zeta_{\text{He}} \leq 4 \times 10^{-18} [1 + 2.8 \times 10^{-3} y n(\text{H I})] \text{ sec}^{-1}. \quad (7)$$

For $y = 5$, this gives an upper limit on ζ_{He} which varies between 7×10^{-18} and $1 \times 10^{-17} \text{ sec}^{-1}$ as $n(\text{H I})$ varies between 50 and 700 cm^{-3} — the limits obtained above. The larger figure agrees with the lower limit on cosmic ray flux computed by Spitzer and Tomasko (1968), and therefore contradicts the result of Hjellming et al. (1969) based on pulsar observations, but as the lifetime of the metastable state is not well known, one must not take this discrepancy too seriously.

d) Interstellar C^{13}H^+

As mentioned earlier, a new interstellar line has been detected just to the blue of $\text{CH}^+ \lambda 4232$. It cannot easily be ascribed to a high velocity component of the common isotopic species and is probably the $\lambda 4232 \text{ \AA}$ line of C^{13}H^+ (Bortolot and Thaddeus 1969). This line was sought first by Wilson (1948) and more recently by Augason and Herbig (1967) to determine the important isotopic abundance ratio $a = [\text{C}^{12}]/[\text{C}^{13}]$. The terrestrial value of this ratio is $a = 89$, while the equilibrium value in the CNO bi-cycle is $a \approx 4$ (Fowler, Caughlan, and Zimmerman 1967). It has been known for some time that a

comparably low ratio is observed in a number of low temperature carbon stars (McKellar 1965). From a synthesis of three spectra (also of ζ Oph obtained with the 120-inch coude spectrograph) Augason and Herbig were able to set an upper limit of 1.5 mÅ for the equivalent width of this line. This limit yielded a $a > 30$, suggesting that the C^{13} -rich carbon stars contributed little to the interstellar medium in the direction of ζ Oph.

The isotope shift is a sum of two components. The first is the difference in vibrational level energies due to the change in molecular reduced mass, and the second is the electronic shift, which is generally much smaller. From Herzberg (1950, Equations III, 195 and III, 203), the isotope shift of a diatomic molecule may be written

$$\Delta\lambda = \lambda^2 \left\{ (1-\rho) \left[\omega'_e \left(v' + \frac{1}{2} \right) - \omega''_e \left(v'' + \frac{1}{2} \right) \right] - (1 - \rho^2) \right. \\ \left. \times \left[\omega'_e x'_e \left(v' + \frac{1}{2} \right)^2 - \omega''_e x''_e \left(v'' + \frac{1}{2} \right)^2 \right] + (1-\rho^2) \left[B'_v J'(J'+1) - B''_v J''(J''+1) \right] \right\}, \quad (8)$$

where $\rho^2 = 0.994022$ is the ratio of the normal to the isotopic reduced mass, and cubic and higher terms and the electronic shift

are neglected. Following the usual convention, ' refers to the upper and '' to the lower state. Herzberg (1950) gives

$$\omega_e'' - 2(\omega_e'' x_e'') = 2739.54 \text{ cm}^{-1}$$

$$\omega_e' = 1850.02$$

$$\omega_e' x_e' = 103.93$$

and $B_0 = 11.43$.

The quantity $\omega_e'' x_e''$ is unknown for CH^+ , but we will adopt the value 49 cm^{-1} , which is $\omega_e'' x_e''$ of B^1H and must be close to the actual value. Thus, from Equation (8), we have $\Delta\lambda = -0.255 \text{ \AA}$. The more recent molecular constants of Douglas and Morton (1960) yield the same result.

The electronic shift between C^{12}H^+ and C^{13}H^+ is small. According to Douglas (1972, private communication), it should be less than 15 percent of the isotope shift computed above. He also estimated that the errors in calculating the usual isotope shift (that is, Equation (8)) are about as large as the electronic shift. The sum of these smaller effects, however, amounts to a total error of less than one line width and may be neglected.

Figure 3 shows the results of the present synthesis in the vicinity of the $\lambda 4232 \text{ \AA}$ line. The strong C^{12}H^+ line falls at $-15.0 \text{ km sec}^{-1}$. Taking the isotope shift computed above, the new line falls at $-15.2 \text{ km sec}^{-1}$ with an equivalent width equal to $0.4 \pm 0.13 \text{ m\AA}$.

The signal strength is over three times the standard deviation of the noise in the filtered spectrum, so there is little doubt that the feature is real. It is hard to see how it could result from an adjacency effect, and in any case no spurious line of this nature has been observed in the vicinity of the other strong lines. We must, however, consider seriously the possibility that the new line is simply a high velocity component of the C^{12}H^+ line. It has been noted that the H and K lines are double at high dispersion, with a high velocity component at -29 km sec^{-1} . This velocity corresponds to a -0.19 \AA displacement from the C^{12}H^+ line, more than a linewidth short of the new feature. Thus it is implausible that the line which we attribute to C^{13}H^+ is produced wholly in the -29 km sec^{-1} cloud, although the possibility that it is blended with a line at this velocity cannot be entirely discounted. Hobbs (1964, private communication), with his Pepsios spectrometer has observed a weak component of sodium D_2 at $-31.6 \pm 0.2 \text{ km sec}^{-1}$. A molecular cloud of this velocity would produce a line at -0.25 \AA with respect to C^{12}H^+ , virtually at the wavelength of the new feature.

We reject this idea, however, on the grounds that it would require an interstellar CH^+/Na density ratio far in excess of any so far observed. Both the new line and Hobb's $-31.6 \text{ km sec}^{-1}$ sodium line ($W \approx 1 \text{ m}\text{\AA}$) are undoubtedly unsaturated, and the ratio of equivalent widths $W(\text{CH}^+)/W(\text{Na I}) \approx 1/2$ is therefore the ratio of optical depths. On the other hand, in the -15 km sec^{-1} cloud this ratio is $1/65$ (Herbig 1968), typical for those clouds where $\lambda 4232 \text{ \AA}$ is conspicuous, although there are admittedly few clouds where the curve of growth is well enough known to permit this ratio to be calculated precisely. However, by taking a reasonable range of values for the doppler constant b , say 1 to 4 km sec^{-1} , it is possible to extract approximate values of $\tau(\text{CH}^+)/\tau(\text{Na I})$ from available data. Thus, for 34 of the 61 stars for which $W(\text{CH}^+)$ has been measured or estimated by Adams (1947) or by Rogerson, Spitzer, and Bahng (1959), $W(\text{Na I})$ is also found in the various compilations of interstellar Na I and Ca II lines (Merrill et al. 1937; Spitzer 1948; Beals and Oke 1953; Münch 1957). Among these, there are a dozen cases where the structure of the D, or H and K, lines suggests that the absorption takes place in essentially a single cloud, in which the CH^+ line is presumed formed, on the basis of common radial velocities. In all these cases, $W(\text{CH}^+)/W(\text{Na I}) < 1/5$, while if the high degree of saturation in the D_2 line is taken into consideration, the optical depth ratio becomes markedly smaller, $\tau(\text{CH}^+)/\tau(\text{Na I})$

$< 1/17$, assuming b in the range 1 to 4 km sec⁻¹. While further investigation of this ratio is indicated, the data just cited are sufficiently extensive to suggest strongly that $\lambda 4232.08 \text{ \AA}$ is unlikely to be a high velocity component of the C¹²H⁺ line, and we instead assign this new feature, on the basis of its precise location at the expected isotope shift, to the species C¹³H⁺.

A potentially conclusive test for the existence of C¹³H⁺ in the -15 km sec⁻¹ cloud would be detection of the equivalent line at $\lambda 3958 \text{ \AA}$, which is the CH⁺ R(0) line of the (1, 0) band in the same electronic system. The isotope shift of this line is +0.44 \AA and there can be no confusion with known high velocity clouds. The Franck-Condon factor for this band is favorable, being roughly half that of the $\lambda 4232 \text{ \AA}$ band according to Herbig (1968). No such line is found, but the upper limit at the wavelength indicated is 0.25 m \AA , consistent with the idea that such a weak line as expected is just below the threshold of detectability. The same situation holds for C¹³N.

The optical depths of the C¹²H⁺ and C¹³H⁺ lines are $\tau_{12} = 0.968$ and $\tau_{13} = 0.012 \pm 0.003$ from the curve of growth. If we rather pessimistically assume that a third of the C¹³H⁺ line may be due to a blend with the stronger line, then $\tau_{13} = 0.012 (+0.003, -0.007)$ and the abundance ratio in the line of sight is

$$a = \tau_{12} / \tau_{13} = 81 (+113, -16) \quad . \quad (8)$$

Recent observations of interstellar CO and C¹³O and ζ Oph have yielded a comparable value of a (Smith and Stecher 1971). Our finding that a is essentially terrestrial in the -15 km sec^{-1} cloud clearly suggests that C¹³-rich stars have not contributed to the CH⁺ molecules, or presumably to the rest of the interstellar matter, in the direction of ζ Oph, and moreover it implies that the composition of the interstellar medium has remained rather stable for the age of the solar system, or 5×10^9 years.

III. THE + 13 KM/SEC⁻¹ CLOUD IN ζ PERSEI

The Perseus II association of which ζ Per is a member has been studied in considerable detail (see Lynds (1969) for references), but the interstellar line spectrum of ζ Per, though extensive at + 13 km sec⁻¹, has received relatively little attention until recently. The high resolution Fabry-Perot work of Hobbs (1969 and 1972, private communication) has resulted in a fairly good idea of the curve of growth and White (1972) has possibly detected Ca I λ 4227 Å with the coudé scanner of the 100-inch telescope at Mt. Wilson. Since the position of the + 13 km sec⁻¹ cloud relative to ζ Per and the other stars in the association is uncertain, it is difficult to establish the ionization equilibrium. Even so we may to some extent proceed as we did for ζ Oph and make an attempt to determine some of the physical conditions and abundances in the cloud.

a) Observational Results

Seven high dispersion spectrograms, similar to the ζ Oph plates described earlier, were obtained with the 120-inch telescope and its coudé spectrograph. The long wavelength half of four of these was not in proper focus due to a maladjustment in the spectrograph, and were not analyzed. The good spectrograms were reduced

to intensity versus wavelength and synthesized by the method described above and in Appendix A.

The observed atomic and molecular line profiles are shown in Figures 10 and 11, and the vicinity of the CN lines in Figure 12. Three of the atomic lines are seen in ζ Per for the first time. These are Fe I $\lambda 3720$ and $\lambda 3860$ Å and Ca I $\lambda 4227$ Å, and all fall at $+13$ km sec⁻¹, the velocity of the strong interstellar lines. Although Ca I $\lambda 4227$ Å is barely detected, it is noteworthy that the line is also observed by White (1972), with the same equivalent width. The strong H and K lines of Ca II appear triple at this dispersion with the main component at $+13$ km sec⁻¹ and weaker lines at -6 and $+21$ km sec⁻¹. The $\lambda 3303$ Å D' lines of Na I show similar structure on four 120-inch coude spectrograms kindly provided by Dr. L. Kuhl. Table 6 lists the equivalent widths and optical depths of all lines detected in the spectral interval $\lambda\lambda 3650-4350$ Å. This table includes as well upper limits to lines in the CH, CH, and CH⁺ bands, of interest in the measurement of the microwave background radiation, and to the Al I $\lambda 3944$ Å line from which an upper limit to the aluminum abundance will be derived.

As in the case of ζ Oph there appears to be no systematic difference between atomic and molecular radial velocities. The

slight inaccuracy in the CH^+ $\lambda 3958 \text{ \AA}$ laboratory wavelength suspected in ζ Oph seems to be confirmed in this cloud.

The curve of growth in the $+ 13 \text{ km sec}^{-1}$ cloud determined from the synthesis alone is quite uncertain. The doublet ratio method yields $b(\text{Ca II}) = 2.1 \text{ km sec}^{-1}$ for the H and K lines, while $b(\text{Na I})$ calculated from the D' lines is 0.7 km sec^{-1} . This discrepancy is only partially explainable by errors in the equivalent widths. The sodium doppler constant may also be obtained from the ratio of the D_1 to the D'_1 line (Strömgren 1948); Hobbs (1969) gives $W(D_1) \approx 140 \text{ m\AA}$, so that $b(\text{Na I}) = 1.6 \text{ km sec}^{-1}$. Unfortunately, the relatively poor agreement between photographic and photoelectric equivalent widths makes the second calculation uncertain. However, the lower value, 0.7 km sec^{-1} , is found also for the CH doppler constant computed for the $\lambda 3886$ and $\lambda 4300 \text{ \AA}$ lines using the electronic f-values of Fink and Welge (1967) and the Franck-Condon factors given by Herbig (1968). The CH doppler constant is strongly affected by uncertainties in the f-values and may be as high as 1.5 km sec^{-1} . Hobbs (1972, private communication) has, however, resolved CH^+ $\lambda 4232$ and reports its doppler constant to be 1.98 km sec^{-1} , corrected for instrumental profile and saturation. We will adopt this value for all the molecules. To sum up, the atomic and molecular column densities (Tables 7 and 8) have been computed from the curve of growth with the doppler constants 2.1 km sec^{-1} for Ca II, 0.7

km sec⁻¹ for Na I, and 1.98 for the molecules. For the faint lines, no curve of growth correction is necessary.

b) The Electron Density and the Atomic Abundances

Owing to a lack of very definite knowledge about the location of the +13 km sec⁻¹ cloud with respect to ζ Per, it is difficult to specify the radiation field at the cloud center. There are some grounds, however, for placing the cloud at a considerable distance from ζ Per. The following arguments are based primarily on the observational data summarized by Lynds (1969).

Galaxy counts in the region of the Perseus II association (Shane and Wirtanen 1967) indicate three regions of different obscuration. Of the six Perseus II stars in Adam's (1949) survey which show molecular absorption, three — ζ Per, X Per, and o Per — fall in the region of highest extinction. These exhibit a significantly different CH⁺/CH line ratio from the three stars which fall outside — ξ Per, HD 22951, and HD 24131. It is reasonable to associate the molecules observed in ζ Per and the other two stars with this high extinction region, and on the basis of their radial velocity, it is reasonable to assume that the atomic lines are formed there as well. According to Lynds (1969), the best estimate of the distances of the heavily obscuring material is 200 — 300 pc from the sun while the association is believed to lie some 300 to 400 pc away. Thus, the cloud and the stellar association which contains ζ Per may be 100 pc or more apart.

Of the three stars lying behind the obscuring layer, the nearest is \circ Per. The distance moduli determined by Blaauw and Borgman (1963), 7.59 mag for ζ Per and 6.48 mag for \circ Per, correspond to distances of 340 and 190 pc. According to Stothers (1972 private communication) ζ Per is a peculiar supergiant and its absolute visual magnitude may be in error by as much as 0.5 mag, but even so, the large difference in distance moduli between the two stars retains some significance. Most likely then, the nearest hot star to the cloud under study is \circ Per (MK type B1III). If \circ Per is 190 pc from the sun, then it is at least 13 pc from the column seen against ζ Per.

We may now proceed to estimate the radiation field at the cloud center. As before, we adopt as a lower limit on the radiation field the diffuse galactic field proposed by Habing (1968), attenuated by the cloud. As an upper limit we take the sum of this field and that of \circ Per at 13 pc, attenuated to a lesser extent since we have really no idea of the extinction between this star and the cloud center. For the total extinction we adopt 0.54 mag at $\lambda 5480 \text{ \AA}$, half that measured by Bless and Savage (1970), and combine their ζ Per reddening curve (that of ζ Oph is used at wavelengths above their region of measurement) with the Witt and Lillie (1971) albedo data to obtain the attenuation factor. To compute the stellar field attenuation we will adopt the smaller extinction value 0.27 mag since the extinction between the cloud center and \circ Per may be smaller than that along the line of sight. The line-blanketed B2II-III

model of Van Citters and Morton (1970) provides suitable fluxes for calculation of the stellar field. The stellar radius is taken to be $13 R_{\odot}$. The atomic photoionization rates for the two fields adopted are given in Table 9.

Assuming the existence of Ca I $\lambda 4227 \text{ \AA}$, the Ca I/Ca II line ratio yields an electron density in the range 0.044 to 0.14 cm^{-3} . Further observations are obviously needed to substantiate this result. The neutral hydrogen densities indicated by this range of n_e may be read from Figure 5. For $\zeta = 1.17 \times 10^{-15} \text{ sec}^{-1}$, $n(\text{H I})$ lies between 10 and 80 cm^{-3} , if carbon is depleted by a factor no greater than 10.

The total column densities of the atoms found in the $+13 \text{ km sec}^{-1}$ cloud are given in Table 10. Since all the elements are presumed to be predominately once-ionized, their relative abundances will probably not change greatly if the electron density found above is in error. It is of some interest to compare the relative abundances observed here and in $\zeta \text{ Oph}$. $N(\text{H I})$ has not yet been measured against $\zeta \text{ Per}$, so the abundances shown in Table 11 are defined relative to sodium whose fractional abundance relative to hydrogen is known to show little variation in the interstellar medium. The deficiencies in iron, calcium, and aluminum are found to be similar in the two clouds.

IV. THE SPECTRUM OF THE MICROWAVE BACKGROUND RADIATION

The history of the microwave background radiation began in 1948 when Gamow and his coworkers, in the course of their investigation into cosmological element synthesis, first recognized the importance of hot thermal radiation in the early expanding universe (Alpher, Bethe, and Gamow 1948; Gamow 1948). They predicted that a highly red-shifted remnant of this radiation would survive into the present era with its blackbody spectrum intact, and made estimates of its temperature falling in the range $5 - 28^\circ \text{K}$ (Alpher and Herman 1949, 1951). Although it is conceivable that this radiation could have been detected with the radio receivers of the day, no deliberate search was attempted until nearly two decades later.

At the suggestion of Dicke in 1965, Roll and Wilkinson at Princeton started to construct a 3.2 cm receiver for detection of Gamow's radiation. In the meantime, while calibrating the 20-foot horn antenna of the Bell Telephone Laboratory at Holmdel, New Jersey, Penzias and Wilson (1965) discovered an excess antenna noise at $\lambda 7.35 \text{ cm}$ which corresponded to a temperature of about 3.5°K . This noise, to their experimental accuracy,

was isotropic and unpolarized, and showed no time dependence.

Their discovery and its interpretation were published in the spring of 1965 (Penzias and Wilson 1965; Dicke, Peebles, Roll and Wilkinson 1965).

The first confirmatory evidence that the radiation had the predicted blackbody character came with the realization that the classical CN observations of Adams (1941) implied $\sim 3^\circ$ K radiation at $\lambda 2.6$ mm. This was rapidly followed by Roll and Wilkinson's (1966) $\lambda 3.2$ cm measurement, which yielded a brightness temperature of $3.0 \pm 0.5^\circ$ K, and a series of further direct measurements that established the blackbody character ($T_B \approx 2.7^\circ$ K) of the radiation over more than two decades of wavelength, from $\lambda 73.5$ cm to $\lambda 3.3$ mm (see Thaddeus 1972 for references).

A crucial region of the spectrum is near 1 mm wavelength, where $\sim 3^\circ$ K radiation has its peak and most of the energy lies. This region is inaccessible from the ground because of the opacity of the atmosphere, but in the past four years there have been direct observations with rockets and balloons from above the atmosphere. These observations disagree among themselves to a great extent and have led to considerable controversy concerning the intensity and shape of the background spectrum. The measurements from the interstellar molecular bands, which concern us here, are

conservative in nature and are not dependent on the accuracy of large instrumental and atmospheric corrections. Although the effect of the curve of growth correction on the molecular upper limits is in fact substantial, it is rather accurately known and any error in it is more likely to still further lower the upper limits. The molecular bands provide one precise measurement and three fundamental constraints at millimeter and submillimeter wavelengths against which all direct observations must be compared.

Much of the observational material on CN, CH, and CH^+ in ζ Oph described here was analyzed in a preliminary way by Bortolot et.al. (1969). Some additional plates have since been obtained, and the densitometry is completely new and more refined. The analysis has further benefitted from a better curve of growth and a more detailed statistical treatment of upper limits to missing lines.

If the CN excitation observed is indeed due to a universal back-radiation, it must show directional invariance. The data available regarding this will be discussed at the conclusion of this section.

a) The Molecular Excitation Temperatures

The excitation temperature of a molecular band may be determined directly from the intensities of any two absorption lines that do not share a common lower level, providing the populations can indeed be described by a single temperature. Consider two

optical absorption lines which arise from transitions from electronic ground state levels i and j ($E_i > E_j$) to excited electronic levels i' and j' . The transition intensities will be proportional to n_i and n_j , the populations of levels i and j . Alternatively, the population ratio may be inferred from the observed line strengths, being given by

$$\frac{n_i}{n_j} = \frac{g_i S_{jj'} \tau_{ii'}}{g_j S_{ii'} \tau_{jj'}} \quad (9)$$

where the g 's are the statistical weights of the levels, the S 's the theoretical line strengths (the summed squared transition matrix elements), and the τ 's the optical depths of the lines. If we define $s = g_j S_{ii'} / g_i S_{jj'}$ and $r = \tau_{ii'} / \tau_{jj'}$, then $n_i / n_j = r/s$ and the excitation temperature is given by

$$T_{ij} = h\nu_{ij} / k \ln(s/r) \quad (10)$$

where h and k are the Planck and Boltzmann constants, and

$h\nu_{ij} = E_i - E_j$. Figure 13 shows partial electronic and rotational — or in the case of CH, fine structure — term diagrams of the three molecules observed optically in interstellar space. The wavelengths at which we will attempt to determine the brightness

temperature of the background radiation are $\lambda 2.64$ and $\lambda 1.32$ mm for CN, and $\lambda 0.56$ and $\lambda 0.36$ mm for CH and CH^+ , respectively.

Direct measurements of the background radiation from high altitude sites may ultimately be made in the $\lambda 1.6$ - 2.6 mm radio window, but these will undoubtedly be extremely difficult. There does not appear to be any prospect of direct measurements from the ground at $\lambda \leq 1$ mm.

The requisite line strength ratios s are obtained for CN and CH^+ from the Hönl-London factors (see Herzberg 1950, p. 208):

$$s = \frac{J_i + J_i' + 1}{J_j + J_j' + 1} \quad (11)$$

where the J 's are the total angular momenta of the levels indicated by subscripts. The CH^+ ground state is $^1\Sigma$; that of CN is $^2\Sigma$, but the doublet splitting is unresolved optically, and Equation (11) is valid. In the case of CH, which is intermediate between Hund's cases (a) and (b), the calculation is somewhat more involved. It requires a transformation of the matrix elements of the electric dipole moment operator, calculated in the pure Hund's case (b) representation, to the intermediate

representation where the molecular Hamiltonian matrix is diagonal. In Hund's case (b) one finds $s = 5/3$, while the correct transformed value is $s = 1.524$.

The likelihood that any pumping mechanism for CN or CH^+ exists which can lower T_{ij} below $T_B(\nu_{ij})$ would appear slight for several reasons: the rotational level schemes are simple, the radiative lifetimes of the levels are short, and the density of the molecular clouds observed optically is probably not great ($\leq 10^3 \text{ cm}^{-3}$). The fine structure selection rules of CH might permit pumping to occur under certain conditions. However, in the clouds where CH is observed the departure of the population ratio from that expected when the pumping is ignored is estimated to be no more than one part in 10^5 (Clauser 1970). Thus local processes such as collisional impact with charged and neutral particles or resonance scattering of starlight can serve only to increase the molecular excitation. The excitation temperatures, therefore, are almost certainly reliable as upper limits to the background brightness temperature.

The observational data on the molecules in the ζ Oph -15 km sec^{-1} cloud have been given in § II b and are shown again for convenience in Table 12. The errors in the CN equivalent widths represent one standard deviation. The optical depths were computed using the CN doppler constant, $b = 1.36 \text{ km sec}^{-1}$, measured by Hegyi et al. (1972).

The CN excitation temperatures, as calculated with Equation (10), are given in Table 13. If we make the minimum curve of growth correction (the observed R(0) line width in the synthesis sets the upper limit 2.40 km sec^{-1} on the doppler constant), the resulting T_{10} (CN) from the R(1)/R(0) and P(1)/R(0) line ratios, $2.99 \text{ }^\circ\text{K}$, is a strict upper limit to the brightness temperature at $\lambda 2.64 \text{ mm}$. The proper curve of growth correction reduces this temperature by a small amount. A correction for the local processes in the -15 km sec^{-1} cloud, also fairly small, converts T_{10} (CN) to T_B ($\lambda 2.64 \text{ mm}$), as discussed immediately below. It is quite difficult to assign an uncertainty to the curve of growth correction, but reasonable limits on the doppler constant indicate that this uncertainty is no larger than those which result from statistical errors in the equivalent width measurements or from the collisional correction. For this reason no uncertainty is assigned. The final weighted mean

$$T_B(\lambda 2.64 \text{ mm}) = 2.75 \pm 0.10^\circ \text{ K} \quad (12)$$

may well be the most accurate determination of the background radiation temperature wavelength at any wavelength.

Table 14 gives the upper limits to the background temperature and intensity at $\lambda \lambda 1.32, 0.56, \text{ and } 0.36 \text{ mm}$ derived from the upper limits in Table 12 and these limits are plotted in Figures 14 and 15.

b) CN Excitation by Local Processes

Although the ground state of CN is $^2\Sigma$, the small ρ doubling of the levels, resolved in the $\lambda 2.6$ mm radio lines (Jefferts, Penzias, and Wilson 1970), is too small to be resolved optically, and therefore on the basis of spectroscopic stability, we may proceed as if the ground state were $^1\Sigma$ and the level structure that of a simple rigid rotator, as shown in Figure 13. Only the two lowest rotational levels are observed to be populated in interstellar space, so that the fractional level populations n_0 , n_1 in statistical equilibrium are determined from the rate equation

$$\frac{dn_1}{dt} = -n_1(C_{10} + A_1) + n_0 C_{01} = 0 \quad , \quad (13)$$

where A_1 is the spontaneous radiative decay rate of the $J = 1$ level

$$A_1 = \frac{64\pi^4 \mu^2 \nu_{10}^3}{9hc^3} = 1.19 \times 10^{-5} \text{ sec}^{-1} \quad , \quad (14)$$

$\mu = 1.45 \times 10^{18}$ esu is the CN dipole moment, and $\nu_{10} = 1.13 \times 10^{11}$ Hz. C_{10} is the radiative or collisional deexcitation rate from the $J = 1$ directly to the $J = 0$ level, while C_{01} is the excitation rate from the $J = 0$ level to all others since the radiative cascade from higher levels to $J = 1$ occurs quite rapidly.

Since the transition cross-sections for $\Delta J > 1$ in neutral particle

collisions will be comparable to those for $\Delta J = 1$, C_{01} and C_{10} will not satisfy detailed balance,

$$\frac{C_{01}}{C_{10}} = \frac{g_1}{g_0} \exp\left(-\frac{h\nu_{10}}{kT_k}\right), \quad (15)$$

where $g_0 = 1$, $g_1 = 3$, and T_k is the kinetic temperature. Nonetheless, while the neutral particle excitation rate may only be estimated, those due to electron and ion collisions are quite accurately known and do obey the radiative selection rules, $\Delta J = \pm 1$, to a good approximation. Thus in the following treatment of collisional excitation it is permissible to proceed as if Equation (15) were valid. Since in the absence of local processes

$$n_1/n_0 = \left(g_1/g_0\right) \exp\left(-\frac{h\nu_{10}}{kT_B}\right) \quad T_B = 2.8^\circ \text{K}, \quad (16)$$

Equation (13) may be solved for the excitation rate. Thus

$$\begin{aligned} C_{01} &= \left(g_1/g_0\right) A_1 \exp\left(-\frac{h\nu_{10}}{kT_B}\right) \left[1 - \exp\left(-\frac{h\nu_{10}}{kT_B}\right)\right]^{-1} \\ &= 6.1 \times 10^{-6} \text{ sec}^{-1}. \end{aligned} \quad (17)$$

This is the rate which is necessary to account for the observed CN excitation.

One may also determine the correction necessary to convert the observed T_{10} to T_B if the excitation rate from local interstellar

processes is known. Since $\exp(-h\nu_{10}/kT_k)$ will always be very close to unity we may set $C_{01}/C_{10} = 3$ and Equations (13) and (16) (where T_{10} replaces T_B) then yield

$$T_{10} = h\nu_{10}/k\theta_n \frac{3A_1 + C_{01}}{C_{01}} \quad (18)$$

If R_{01} is the excess of C_{01} over $6.1 \times 10^{-6} \text{ sec}^{-1}$, this gives

$$\Delta T_{10} = -2.0 \times 10^5 R_{01} \text{ } ^\circ\text{K} \quad , \quad (19)$$

where ΔT_{10} is the temperature correction computed for $T_{10} \approx 3 \text{ } ^\circ\text{K}$ and R_{01} is on the order of $6 \times 10^{-6} \text{ sec}^{-1}$ or smaller.

We will now consider the rates expected in the CN clouds which can contribute to the CN excitation, first to see whether any process besides photoexcitation by background radiation can account for the observed excitation, and secondly to determine what correction to $T_{10}(\text{CN})$ must be made to obtain $T_B(\lambda 2.64 \text{ mm})$. The processes most likely to be of consequence are (1) collision of CN with neutrals, primarily H I, but possibly H_2 and He; (2) collisions with electrons; (3) collision with protons, if the CN happens to lie on the edge of an H II region; and (4) optical photoexcitation by starlight. Vibrational excitation of CN either by photons or collisions is too slow to be significant and need not be considered.

i) Neutral Particle Collisions

While the excitation cross-sections for neutral particles on CN are not well known at present, they cannot greatly exceed the geometrical cross-section, which we take to be $\sigma_{01} \sim 2 \times 10^{-15} \text{ cm}^2$. In the -15 km sec^{-1} cloud we have concluded that $n(\text{H I})$ is less than 300 cm^{-3} . Assuming an upper limit on projectile velocity $v = 1.2 \times 10^5 \text{ cm sec}^{-1}$ (for 100° K H-atoms), therefore, one obtains

$$C_{01} = n(\text{H I}) v \sigma_{01} \leq 1.6 \times 10^{-7} \text{ sec}^{-1}, \quad (20)$$

a rate smaller than that required by a factor of about 40. If the effects of He I, taken at normal cosmic abundance, and H_2 , which, as Carruthers (1970) has suggested, is perhaps as abundant as H I, are included, C_{01} increases by a factor less than 2. Hence almost certainly, neutral particle impact is not the cause of the CN excitation.

If there were a sufficient H I density to account for T_{10} , then the CO excitation temperature (Smith and Stecher 1971) and probably the optical extinction would be much greater than observed.

ii) Electron Impact

The long range of the Coulomb interaction makes electron impact a highly effective process for rotationally exciting polar molecules; the rate coefficient is a factor of roughly 10^5 greater than that for neutral particles at H I region kinetic velocities.

Since this process comes closest to accounting for the 2.8 °K excitation, it is fortunate that both electron density in this cloud and the rate coefficient are rather accurately known. As we have mentioned above, n_e in the ζ Oph - 15 km sec⁻¹ cloud is between 0.07 and 0.23 cm⁻³. The rate coefficient has been computed by Allison and Dalgarno (1971) from a close-coupling calculation to be $r_{01} = 2.1 \times 10^{-6}$ cm⁻³ sec⁻¹ for 100° K electrons and at this temperature is quite temperature insensitive. Thus

$$3.4 \times 10^{-7} \leq C_{01} = n_e r_{01} \leq 12.2 \times 10^{-7} \text{ sec}^{-1}, \quad (21)$$

at its maximum only a factor 6 short of the observed rate. While it is thus unlikely that electron impact is able to produce the observed excitation, this process does raise T_{10} by 0.07 to 0.24° K.

iii) Proton Impact

Although rotational excitation by protons in low temperature H I regions is completely negligible, it is considerable in H II regions: Thaddeus (1972) has determined from a close-coupling calculation that a quite moderate density of 10⁴ °K protons, 1.6 cm⁻³, is sufficient to account for the excitation observed. It becomes necessary, therefore, to show that the molecular lines are formed outside H II regions if we are to discard proton impact as the excitation source. As noted in section II, Herbig (1968) has argued convincingly that the - 15 km

sec^{-1} cloud must be an H I region. It is probably safe to conclude that proton collisions, while potentially an effective mechanism for CN excitation, actually do not contribute much to it.

iv) Optical Photoexcitation

Photoexcitation by the general galactic field is of interest as a possible explanation of the directional invariance of $T_{10}(\text{CN})$ which we have noted. The rate is greatest for the violet system, for which

$$C_v = \frac{\pi e^2}{mhc^2} u_\lambda \lambda f \quad (22)$$

(Thaddeus and Clauser 1966) where u_λ is radiation density, $f = 0.027$ is the oscillator strength of the electronic transition (Bennett and Dalby 1962) and λ its wavelength. Zimmermann (1968) gives the galactic field $u_\lambda \approx 57 \times 10^{-18} \text{ ergs cm}^{-3} \text{ \AA}^{-1} \text{ sec}^{-1}$ at $\lambda 3900 \text{ \AA}$ which is much higher than that assumed at the -15 km sec^{-1} cloud center, hence $C_v \leq 8 \times 10^{-10} \text{ sec}^{-1}$. It is obvious that this process has virtually no effect on the CN excitation.

Of course, light from a nearby star, in particular the OB star against which the molecules are typically observed, could increase this rate drastically, but there would then be no reason to expect the CN excitation to be invariant, as it is observed to be, and furthermore the intense UV of such stars would tend to dissociate

the CN. It would then be difficult to explain the existence of the molecule in interstellar space.

We therefore conclude that no local process in the -15 km sec^{-1} cloud is able to produce the observed $2.8 \text{ }^\circ\text{K}$ CN excitation and that the correction to convert $T_{10}(\text{CN})$ to $T_B(\lambda 2.64 \text{ mm})$ is in fact small ($0.15 \pm 0.09 \text{ }^\circ\text{K}$). The correction necessary in the $\zeta \text{ Per } +13 \text{ km sec}^{-1}$ cloud is smaller still ($0.04 \pm 0.02 \text{ }^\circ\text{K}$).

c) Discussion of the Short Wavelength Observations

Shivanandan (NRL) and Houck and Harwit (Cornell; 1968) made the first attempt to detect the short wavelength background radiation directly from above the atmosphere. Their rocket-borne far-infrared telescope picked up a large flux, apparently isotropic, about 40 times greater than that of a 2.8° K blackbody in the interval $\lambda 1.3$ to 0.4 mm . Two subsequent flights by the Cornell group appeared to confirm this result (Houck and Harwit 1969; Pipher et al. 1971). The mean intensity over the instrumental passband, $5 \times 10^{-14} \text{ erg cm}^{-2} \text{ sec}^{-1} \text{ ster}^{-1} \text{ Hz}^{-1}$, is considerably in excess of the molecular limits given here, especially that derived from CH (see Figures 14 and 15). Thus a radiation continuum is ruled out, and if the radiation is not spurious, it must be concentrated in some linelike feature or features which happen to avoid the molecular resonances. This possibility has prompted other workers to fly experiments with

some spectral resolution for a more detailed look at the excess radiation.

The first such experiment, the balloon-borne radiometer of Muehlner and Weiss (1970), did provide some evidence of a strong line between 10 and 12 cm^{-1} , but all subsequent work has contradicted this result (Mather et al. 1971; Blair et al. 1971). Muehlner and Weiss (1972) have themselves repeated their 1970 experiment with an improved version of their radiometer and report no line.

Although corrected for a quite sizable atmospheric contribution, these new observations of Muehlner and Weiss cast considerable doubt on the existence of any short wavelength background radiation in excess of ~ 3 °K. The new intensities and upper limits are marked M in Figures 14 and 15. The results are all consistent with ~ 3 °K radiation and disagree considerably with the Cornell-NRL measurements. If the new data are taken conservatively as only upper limits, and if the large excess flux seen only in the Cornell-NRL flights is spurious, then one is forced to recognize that there is really only meager evidence for the existence of any short wavelength background radiation.

The molecular upper limits, essentially because, as we have argued, neglected processes can only depress them further, provide the most reliable data on the intensity of the background radiation. It is certainly worth pursuing this direction further. The

shortest wavelength at which the background has been detected with certainty is $\lambda 2.64$ mm from CN, and it would be highly desirable to extend detection to shorter wavelengths. In principle, the technique of plate synthesis could be extended to permit the measurement of the CN R(2) line and hence the intensity at $\lambda 1.32$ mm. Our upper limit is just a factor 2.5 greater than the expected equivalent width. However, the observing time would be large and a more appropriate approach would probably be to make use of photoelectric techniques. Hegyi, Traub, and Carleton (1972) have made the first such attempt to detect the R(2) line in ζ Oph, using a Fabry-Perot spectrometer on a 60-inch telescope. If their result is interpreted in the same manner as the present work, their upper limit is still in excess of the 0.17 mÅ found here, but it is estimated that with a large telescope a week or two of observing time might suffice for the detection of this line.

d) Invariance of the CN Excitation

Since pumping mechanisms are excluded in the two clouds we have studied in detail, and we have no reason to expect pumping in the other clouds observed, the CN excitation temperature found in any of these clouds must be equal to 2.8 °K, if its source is correctly identified with photoexcitation by the microwave background radiation. Such observations provide then a critical test of the hypothesis that the background radiation causes the excitation, and are the primary motive for seeking interstellar

CN in new stars. The existence of the short wavelength background probably collapses if $T_{10}(\text{CN})$ can be found in a single case to be zero, or even appreciably less than 2.8°K .

So far the number of stars against which CN has been observed is small: Adams (1949) in his survey of 300 OB stars found seven, and subsequent workers have reported relatively few more. CN temperatures observed against several stars have been noted by Clauser and Thaddeus (1972) and Peimbert (1968), but only $\zeta \text{ Oph}$ and $\zeta \text{ Per}$ are sufficiently bright and behind enough CN to provide a fairly precise temperature determination. In this section we will refine some of the past measurements and present the results of a search for CN against a number of late B and early A stars.

i) Observational Results

We will first discuss criteria for our choice of objects to observe. Experience has shown that the best place to find CN is against bright OB stars near the galactic plane where most of the interstellar material is concentrated. They have convenient spectroscopic properties, being intrinsically bright and having broad, uncomplicated stellar features as well, so most of the CN temperatures have been measured against them. These stars, however,

suffer from two disadvantages: those whose spectra contain CN are few, and more importantly, tend to be associated with H II regions. If the CN were located, at least in part, at the edge of the ionization region, then the excitation, as noted above, might be affected by collision with thermal (10^4 °K) protons. If the CN lines are not formed unambiguously in H I regions, then the temperatures may be in doubt. Hence stars later than OB, which are free from extensive H II regions, would be preferable as objects for observation. Peimbert (1968) has discovered CN in two or three out of nine later-type stars he investigated.

We have chosen, therefore, two groups of objects for study, (1) certain OB stars known to contain CN, and (2) late B and early A giants with extinction of ~ 0.3 mag or greater. High dispersion spectrograms of the stars listed in Table 15 were obtained with the 120-inch coude spectrograph and reduced as before. Of the seven later spectra, one, that of 13 Ceph, had the strongest CN R(0) line yet seen, excepting two distant objects reported by Münch (1964), and another, that of HR 7573, was found to contain CN weakly.

Except in the cases of ζ Oph and ζ Per, the CN doppler constants are not known and it is necessary to assume a value of b to compute optical depths. In lieu of more precise data we will adopt $b = 1.67 \text{ km sec}^{-1}$, the average value for the ζ Oph and ζ Per clouds. We will not attempt to assign an error due to uncertainty in the curve of growth, but since the CN lines are fairly weak, the curve of growth errors cannot be large compared to uncertainties in local excitation processes and in the equivalent widths themselves. The equivalent widths and corresponding optical depths are given in Table 16.

The rotational excitation temperatures are presented in Table 17 for all stars in Table 15 in which CN is found, except HR 7573, where the R(1) line is not seen with any degree of confidence ($T_{10} < 3.3^\circ \text{ K}$). This table includes some additional objects investigated by Clauser and Thaddeus (1972) and Peimbert (1968). BD+66° 1674 and BD+66° 1675 have been assigned the large doppler constant 5 km sec^{-1} by Clauser and Thaddeus on the basis of their great distance and low galactic latitude. Note should be made that the entries for ζ Per and X Per represent measurements in essentially the same cloud, as pointed out in the previous section.

ii) Discussion

The CN temperatures in these widely separated clouds though less certain than in ζ Oph or ζ Per are all consistent with 2.8° K. This apparent invariance supports the idea of a universal background radiation, but in addition provides what is perhaps the strongest evidence that the molecular lines originate in H I regions and that the excitation mechanism is not "local".

While the effect of fast protons on CN excitation is exceedingly large, the lack of large variations in temperature observed against the early stars, when taken in the context of the great inhomogeneity of the interstellar medium would appear good evidence that the molecules do not exist in ionized regions. This idea is supported by the radial velocity coincidence generally observed between the CN and the 21-cm lines. It is noteworthy that $T_{10}(\text{CN}) \sim 2.8^\circ$ K is obtained for several late-type stars which cannot maintain extensive H II regions.

Although we lack exact knowledge of the physical conditions in most of the clouds observed, it is unlikely that electrons, probably the chief local contributor to the excitation in H I regions, are sufficiently abundant to affect $T_{10}(\text{CN})$ very much. One does not expect that the electron collision temperature

correction will exceed a few tenths of a degree, hence within the accuracy of the measurements one can probably equate $T_B(\lambda 2.64 \text{ mm})$ with $T_{10}(\text{CN})$.

This conclusion is susceptible to a direct test through observation of the CN $\lambda 2.6 \text{ mm}$ radio lines: if the molecules are not in equilibrium with the background radiation then they will be observed in emission, by an amount dependent on the optical depth of the cloud. The molecular radiation temperature may be calculated if the cloud completely fills the antenna beam and has only a moderate optical depth, conditions quite probably fulfilled by the clouds considered here. If there is no background radiation, yet the excitation temperature is observed to be 2.8° K , then the line radiation temperature of the strong transition $F_1 F = 3/2 \ 5/2 \rightarrow \frac{1}{2} \ 3/2$ will be

$$T_R \approx 0.25 \tau_0 (^\circ \text{K}) \quad (23)$$

(Thaddeus 1972) where τ_0 is the optical depth of the line. For $\zeta \text{ Oph}$, where $\tau_0 = 0.34$, $T_R \approx 0.08^\circ \text{ K}$, barely detectable with existing receivers, but for $\text{BD}+66^\circ 1675$, where $\tau_0 \sim 5$, this would be about 1.2° K . Penzias, Jefferts, and Wilson (1972) have, in fact, made a search for the $3/2 \ 5/2 \rightarrow \frac{1}{2} \ 3/2$ line against $\text{BD}+66^\circ 1675$ and find $T_R = 0.036 \pm 0.037^\circ \text{ K}$, essentially a null result supporting the conclusion of the last paragraph.

It may be that this measurement, with the observed excitation temperature, offers the most convincing evidence of the validity of the CN thermometer. Two other stars where the CN optical depth is sufficient to make this sort of search worthwhile are 13 Ceph and 20 Aql.

While based on a small sample and hardly conclusive, the temperature invariance thus far observed is highly indicative that the CN excitation results from a universal mechanism, and not from local interstellar conditions.

V. SUMMARY AND CONCLUSIONS

A large number of high dispersion spectrograms of ζ Oph and ζ Per in the spectral interval $\lambda 3650 - 4350 \text{ \AA}$ have been added together digitally to produce low noise, high resolution spectra. The improvement in signal-to-noise ratio has made possible the detection of six interstellar lines, of Ca I, Fe I, K I and C^{13}H^+ , in ζ Oph, their equivalent widths ranging from 0.3 to 2 mÅ, and three lines, of Ca I and Fe I lines of comparable strength in ζ Per. The syntheses have also provided new upper limits on as yet undetected lines relevant to atomic and molecular abundances — in particular to measurements of the intensity of the microwave background radiation at several millimeter and submillimeter wavelengths.

Ca I $\lambda 4227 \text{ \AA}$, the most important of the newly detected lines, provides a direct determination of the ionization equilibrium and hence the electron density. In ζ Oph this is found to be $n_e = 0.16 - 0.55 \text{ cm}^{-3}$. In ζ Per the existence of the Ca I line is marginal, but if the suspected line is real one finds that $n_e = 0.044 - 0.14 \text{ cm}^{-3}$. The neutral hydrogen density is difficult to determine, but if the upper limit of Spitzer and Tomasko (1968) is adopted for the cosmic ray ionization rate of hydrogen, and the

depletion factor of carbon is assumed to be no greater than 10, then $n(\text{H I})$ in the ζ Oph cloud lies between 50 and 700 cm^{-3} ; in the ζ Per cloud $n(\text{H I})$ lies between 10 and 80 cm^{-3} .

In the ζ Oph cloud sodium and potassium both appear at approximately their normal cosmic abundances relative to hydrogen, but calcium, iron, and aluminum are underabundant by factors of 2500, 300, and > 100 , respectively. The abundances relative to sodium in the ζ Per cloud show substantially the same behavior. These results support the idea that most of the iron, aluminum, and perhaps other elements are contained in the interstellar grains.

A new line at $\lambda 4232 \text{ \AA}$ in the ζ Oph cloud is ascribed to C^{13}H^+ and yields a $[\text{C}^{12}]/[\text{C}^{13}]$ ratio of $81(+113, -16)$. This is close to the terrestrial value 89, and suggests that C^{13} -rich stars have not contributed much to the interstellar medium (at least in the vicinity of the sun) and that the composition of the interstellar medium has changed little in the past 5×10^9 years.

The CN, CH, and CH^+ interstellar bands have yielded a value of the intensity of the microwave background radiation at $\lambda 2.64 \text{ mm}$ and upper limits at 1.32, 0.559, and 0.359 mm. The CN rotational temperature, $T_B(\lambda 2.64 \text{ mm})$, is found to be equal

to 2.75 ± 0.10 °K for ζ Oph and 2.66 ± 0.12 °K for ζ Per. The short wavelength upper limits are consistent with a 2.8° K blackbody spectrum and place constraints on the interpretation of recent rocket and balloon experiments.

Observations for the purpose of obtaining additional CN temperatures were made on two other early-type stars known to have CN absorption, and on two late B and five early A giants, two of which were found to contain CN. The rotational temperatures measured are all consistent with a 2.8° K brightness temperature.

It is interesting to note that no systematic factor of five increase in sensitivity in coudé spectroscopy at the highest dispersion has been obtained since the advent of the coudé spectrograph in the 1930's. Thus the results presented here encourage the belief that a number of new interstellar lines await discovery by the systematic application of new techniques.

APPENDIX A
DENSITOMETRY

Wavelength and intensity calibration and spectral synthesis and filtering were done entirely digitally in the following way. In three successive densitometer scans of a given 10-inch plate the transmission T and displacement x at every 4 microns of plate travel were recorded digitally on magnetic tape for the two Fe comparison spectra and the stellar spectrum. In scanning the stellar spectrum the projected slit length of the densitometer was matched to that of the coude spectrograph so that all useful information was acquired in a single scan. Scans across the intensity calibration bars were next made at three different wavelengths, and all data were then read into the large disk storage of the Goddard Institute IBM 360/95 computer system, with which all subsequent data analysis was done.

By least squares fitting a third-order polynomial expansion of λ as a function of x to about 25 Fe lines in both comparison spectra, an absolute wavelength calibration curve accurate to at least 0.004 \AA over the whole plate was obtained, and this was used to convert T to a function of λ . The relative wavelength calibration from plate to plate was apparently even better

than 0.004 \AA : on correcting for the earth's motion it was found that the wavelength assigned to a given strong interstellar line (e.g. H, K, $\text{CH}^+ \lambda 4232$, $\text{CH} \lambda 4300$) on different plates agreed to about 0.002 \AA , which corresponds in radial velocity to only 0.16 km sec^{-1} , about 3% of the width of the sharpest interstellar lines in the -15 km sec^{-1} cloud. Thus no significant decrease in spectral resolution was to be expected from adding spectra together, and it was indeed found that those strong interstellar lines visible on a single plate showed no increase in width as successive spectra were folded into the final synthesis.

The intensity calibration function is that suggested by de Vaucouleurs (1968) for use in the threshold and toe regions of the characteristic curve:

$$I = A \left(\frac{T_0}{T} - 1 \right)^n \quad (\text{A1})$$

where I is the intensity, T and T_0 are the spectrum and clear plate transmissions in arbitrary units as measured by the densitometer, and A and n are constants determined by a χ^2 fitting procedure. This function has the convenient property that when $\log [(T_0/T) - 1]$ is plotted against $\log I$, a straight line results, simplifying the numerical calculations. Clearly, n may be

identified with the inverse of γ , the slope of the linear part of this characteristic curve, so that this function will be appropriate up to the point where the emulsion begins to saturate ($D > 2$ for Ila-O). The proportionality constant A has no actual importance since in the measurement of equivalent widths, only relative intensities of adjacent points in the spectrum are involved. In principle T_0 could be measured, but in practice adjacency effects and the variation in fogging across some plates make this measurement often rather arbitrary. It was thought, then, that more precision could be obtained by introducing T_0 as a third parameter in the fit. The measurements of the calibration bars from the three scans across the plate were averaged together to obtain a single calibration function rather than being employed to determine a separate calibration for each region of the plate. This procedure is justified by the small variation of the low-density part of the Ila-O characteristic curve with wavelength in the region covered by the spectrograms (Latham 1969; Wright 1969). It is estimated that errors in equivalent width due to photometric reduction are under 4 percent. As a consistency check the strong H and K lines of Ca II were measured on single plates and the rms scatter of these equivalent widths was found to be 5 percent. This figure includes errors due both

to the intensity reduction and to placement of the intensity continuum. Finally, the results for strong lines from this synthesis agree quite well with those obtained by Herbig (see Table 1) with the same spectrograph. This comparison, of course, avoids the notorious discrepancy in equivalent widths measured at different observatories.

Once the stellar spectrum is reduced to normalized intensity versus wavelength, it is corrected for the earth's orbital motion and converted by numerical interpolation to a standard form with uniform spacing (0.005 \AA). It then is added into a cumulative synthesis with a weight inversely proportional to the mean square noise averaged over several 3 \AA intervals, following the usual prescription for maximizing the synthesis signal-to-noise ratio. Since the spectrograms were fairly uniform in quality, this refinement over equal weighting probably gained very little.

APPENDIX B

STATISTICAL ANALYSIS OF UPPER LIMITS

Since some of the more interesting results in this paper are upper limits on the strength of absorption lines, it becomes important to extract the maximum information possible from the synthesis. Here we present a simply statistical method based on the assumption that there is no probability for line emission, that improves to some extent the upper limits obtained from the usual two or three standard deviation criterion without loss of strictness.

First consider the simple case of a rectangular absorption line one data point spacing in width which subtracts ΔI_0 from the continuum at one known wavelength and assume that the continuum has a component of uncorrelated gaussian noise with standard deviation σ . The object of the method is to find, with some arbitrary probability or strictness P , an upper limit s_0 to the true ΔI_0 , given σ and the measured deviation at that wavelength ΔI . The probability density is gaussian:

$$p(\Delta I|s) = (2\pi\sigma)^{-1/2} \exp \left[-(\Delta I - s)^2 / 2\sigma^2 \right] \quad (\text{B1})$$

where s is the hypothetical true value for ΔI_0 . For use in a

hypothesis test, $p(\Delta I|s)$ should be multiplied by the probability density of s , which is assumed zero where s represents emission, but is unknown otherwise. Following the method first applied by Gauss we assume the probability density to be a constant where s would indicate absorption. The probability that s is contained in the interval $\{0, S\}$ is then

$$P(s_0) = \frac{\int_0^{s_0} p(\Delta I|s) ds}{\int_0^{\infty} p(\Delta I|s) ds} \quad (\text{B2})$$

where the denominator provides the normalization. Inversion of this equation gives two cases:

1) $\Delta I \leq 0$ ("absorption")

$$s_0 = \Delta I + \sqrt{2\sigma^2} \operatorname{erf}^{-1} \left[P - (1-P) \operatorname{erf} \left(-\Delta I / \sqrt{2\sigma^2} \right) \right] \quad (\text{B3a})$$

2) $\Delta I > 0$ ("emission")

$$s_0 = \Delta I + \sqrt{2\sigma^2} \operatorname{erf}^{-1} \left[P + (1-P) \operatorname{erf} \left(\Delta I / \sqrt{2\sigma^2} \right) \right] \quad (\text{B3b})$$

As ΔI becomes large negative the expression reduces to the usual one, but as ΔI goes through zero to large positive, s_0 approaches zero asymptotically.

The shape of the sharp interstellar lines is mainly determined by the instrumental profile of the spectrograph, which is to a good approximation, gaussian. Since the plate grain noise is expected to be nearly white, the familiar theorem due to North that the optimal filter of a line in white noise is the line itself will be approximately correct. The filtering procedure adopted was to use the gaussian filter whose width maximized the signal-to-noise ratio of the moderately strong CH^+ lines at $\lambda\lambda 3745$ and 3958 \AA . The resultant filter width (full width at half maximum) was 0.050 \AA compared to the 0.058 \AA measured from the lines and led to about a factor 2 improvement in signal-to-noise for these lines.

In order to determine whether or not this approximate method was valid, we made a statistical analysis of the grain noise. The noise power spectrum of the synthesis was determined by Fourier analysis and found to be a superposition of two more or less gaussian distributions. The first, about five times wider than the transform of the sharpest interstellar lines, is the expected white grain noise already filtered to some extent by the densitometer analyzing slit. The second is of the same amplitude but has about the same width as the line transform: its origin is not completely understood. The general filter function appropriate to the problem at hand is the infinite memory filter of Zadeh and Ragazzini (1952) which has the particularly simple form:

$$q(\lambda) = \int_{-\infty}^{\infty} \frac{\Delta \mathfrak{F}(\omega)}{\Phi(\omega)} e^{i\omega\lambda} \frac{d\omega}{2\pi} \quad (\text{B4})$$

where $\Delta \mathfrak{F}(\omega)$ is the Fourier transform of the observed line profile, and $\Phi(\omega)$ is the noise power as a function of spatial frequency. When $\Phi(\omega)$ is a constant (white noise), $q(\lambda)$ reduces to the line profile. Thus the effect of the narrow noise distribution will be to broaden the filter transform and hence to narrow the filter, as was seen empirically above. Since the sum of the two noise distributions is also very roughly gaussian, the filter will not differ much from the gaussian line shape except in width, and the functional distortion is estimated to be no more than the error involved in assuming the observed lines to be gaussian. Because of this conclusion, and because the major uncertainty in determining upper limits is the placement of the continuum, which is to some extent discretionary, any refinement over the empirical best gaussian filter would have little effect in decreasing upper limits.

The quantities ΔI and σ in the filtered spectrum are determined in the following way. A least squares linear fit is made to a 1 to 2 Å interval containing the expected wavelength of the line for which one desires an upper limit: since the line is not observed it cannot affect the continuum fit. The difference

ΔI , between the continuum and the measured intensity at the appropriate wavelength, and the rms error of the fit σ are used in Equations (B3) to obtain an upper limit on line depth. The corresponding equivalent width upper limit is related to this by a constant of proportionality deduced from the weaker observed lines. The strictness criterion $P = 0.99$ in Equations (B3) was chosen for a confidence level of 99 percent.

APPENDIX C

STATISTICAL ERRORS IN EQUIVALENT WIDTH MEASUREMENT

Once we have characterized the noise by its power spectrum, or the fourier inverse of the power spectrum, the autocorrelation function, it is not difficult to determine the standard deviation of the equivalent width integral. This will be the product of the range of integration and the rms error of the mean continuum computed over that interval. Let the integration range Λ comprise N points spaced evenly $\delta\lambda$ apart, and σ^2 be the variance of the noise, normalized to unity continuum. For simplicity, the continuum is shifted to zero.

The variance of the mean continuum is then given by

$$\sigma_M^2 = \frac{\sigma^2}{N} + \frac{2}{N} \sum_{k=1}^{N-1} \left(1 - \frac{k}{N}\right) R(k\delta\lambda) \quad (C1)$$

(Davenport and Root 1958, p. 80), where $R(\lambda)$ is the autocorrelation function of the noise. When the noise is uncorrelated over the sampling period, $R(\lambda)$ approaches a delta function and the second term makes no contribution. The variance of the mean is then σ^2/N , the result expected for the average of N statistically independent points. When the noise is highly correlated, however, $R(\lambda)$ is nearly a constant, equal to σ^2 (since $R(0) = \sigma^2$), over the range of integration, and one

has $\sigma_M^2 = \sigma^2$. Any single point measurement is as good as an average of adjacent highly correlated points.

The noise autocorrelation function for the ζ Oph synthesis is to a good approximation

$$R(\lambda) = \sigma^2 \left\{ \frac{6}{7} \exp\left[-\lambda^2/2(0.005 \text{ \AA})^2\right] + \frac{1}{7} \exp\left[-\lambda^2/2(0.029 \text{ \AA})^2\right] \right\} \quad (C2)$$

For $N = 24$, or $\lambda = 0.120 \text{ \AA}$, more than 99 percent of the equivalent width is included in the integral. From equation (C1) we have

$$\sigma_M = 0.40\sigma \text{ or } \sigma_W = 48\sigma \text{ m\AA}.$$

TABLE 1. INTERSTELLAR LINES IN ζ OPHIUCHI IN
THE REGION

$\lambda\lambda$ 3650-4350 Å

Rest Wavelength (Å)	Atom or Molecule	f-value [†]	This Work		Herbig	
			W [‡] (mÅ)	v [§] (km sec)	W (mÅ)	v (km sec ⁻¹)
3719.935	Fe I	0.041 ^h	1.9	-14.9	<3.	
3745.310	CH ⁺		6.0	-15.1	7.2	-15.1
3779.18	CO ⁺	0.00050 ⁱ	<0.20		<3.	
3859.913	Fe I	0.023 ^j	1.0	-15.0	<3.	
3873.369 ^a	CN R(2)		<0.17		<3.	
3873.998	CN R(1)	0.0069 ^k	2.7	15.0	3.4	-13.8
3874.608	CN R(0)	0.0173 ^k	8.2	-15.2	9.2	-14.8
3875.763	CN P(1)	0.0058 ^k	1.4	-15.2	≤2.	-14.9
3878.768	CH	0.00047 ^l	2.0	-14.5	3.	-13.3
3886.410 ^b	CH	0.0014 ^l	5.7	-15.1	5.9	-14.4
3888.646 ^b	He I	0.064 ^m	<0.25		<3.	
3890.213	CH	0.00093 ^l	3.7	-14.7	5.6	-14.3
3933.664	Ca II	0.69	34.8 9.8	-15.1 -29.1	34.2 10.1	-15.0 -29.0
3944.016 ^c	Al I	0.115	<0.26		<3.	
3957.700	CH ⁺		14.8	-15.7	13.3	-15.4
3758.14 ^d	C ¹³ H ⁺		<0.25		<3.	
3968.470	Ca II	0.344	20.6 4.7	-14.8 -28.8	21.3 5.4	-14.2 -28.0
3999.08	CO ⁺	0.00052 ⁱ	<0.23		<3.	
4044.145 ^b	K I	0.0061	0.8	-15.3	<3.	
4047.213	K I	0.0031	0.3	-15.0	<3.	
4119.48	SiH		<0.22		<3.	
4226.728	Ca I	1.75	1.3	-15.8	<3.	
4229.337 ^e	CH ⁺ R(1)		<0.22		<3.	
4232.28 ^f	C ¹³ H ⁺		0.4	-15.2	<3.	
4232.539	CH ⁺ R(0)		24.3	-15.0	27.4	-14.0
4250.94	CO ⁺	0.00056 ⁱ	<0.28		<3.	
4300.321	CH R ₂ (1)	0.0052 ^l	19.6	-16.0	20.5	-14.6
4303.947 ^g	CH R ₁ (1)		<0.28		<3.	

* Except where noted, all rest wavelengths are from Herbig (1968).

† Except where noted, all atomic f-values are as given by Wiese, Smith, and Miles (1969).

‡ Upper limits represent a confidence level of 99 percent.

§ Heliocentric velocity of line centroid.

|| Velocity of line peak.

Notes to Table 1.

- a. Jenkins and Wooldridge (1938).
- b. Moore (1945).
- c. Burgess, Field, and Michie (1960).
- d. Bortolot and Thaddeus (1969).
- e. Douglas and Herzberg (1942).
- f. This work (see § IID).
- g. Gerö (1941).
- h. Bridges and Wiese (1970).
- i. Herbig (1948), Table 12.
- j. Corliss and Bozman (1962), scaled to (h).
- k. Herbig (1968), Table 9.
- l. ibid., Table 8.
- m. Osterbrock (1964).

1-a

A

TABLE 2. ATOMIC COLUMN DENSITIES IN THE
 (OPH -15 KM SEC⁻¹ CLOUD

atom	$\lambda(\text{\AA})$	$N(\text{cm}^{-2} \times 10^{-11})$
Fe I	3719.935	3.8
	3859.913	3.3
Ca I	4226.728	0.047
Ca II	3933.664	
	3968.470	4.8*
K I	4044.145	9.1
	4047.213	6.8
Al I	3944.018	<0.6
He I	388.646	<0.3

* Determined by doublet ratio method
 (Strömberg 1948), $b = 1.92$ km/sec.

TABLE 3. MOLECULAR COLUMN DENSITIES IN THE
 ζ OPH - 15 KM SEC⁻¹ CLOUD

Molecule	λ (\AA)	$N(\text{cm}^{-2} \times 10^{-13})^*$
CH	4300.321	2.0
	3890.213	2.3
	3886.410	2.4
	3878.768	2.4
CN	3874.608	0.30
	3873.998	0.23
	3875.768	0.14
SiH	4119.48	<0.04
CO ⁺	4250.94	<3.1
	3999.08	<3.1
	3779.18	<3.2

* Calculated for $b = 1.36 \text{ km sec}^{-1}$.

TABLE 4. ATOMIC PHOTOIONIZATION AND RECOMBINATION
 RATES IN THE ζ OPH - 15 KM SEC⁻¹ CLOUD

Atom	Γ ($\times 10^{11}$) sec ⁻¹		α ($\times 10^{11}$) cm ⁻³ sec ⁻¹
	high field	low field	
Na I	3.96	0.93	0.59 [*]
Al I	81.4	27.8	0.85 [†]
K I	10.4	2.62	0.56 [*]
Ca I	33.6	9.6	0.60 [*]
Fe I	44.2	9.6	0.60 [§]

* Seaton (1951)

† Burgess, Field, and Michie (1960)

§ assumed

TABLE 5. ATOMIC ABUNDANCES IN THE ζ CLOUD
 - 15 KM SEC⁻¹ CLOUD

Atom	N (cm ⁻²)	Fractional Abundances	
		ζ Oph	Solar System (Cameron 1968)
H	4.2×10^{20}	1.0	1.0
Fe	4.3×10^{13}	1.0×10^{-7}	3.4×10^{-5}
Al	1.1×10^{13}	$<2.6 \times 10^{-8}$	3.3×10^{-6}
Ca	4.8×10^{11}	1.1×10^{-9}	2.8×10^{-6}
Na	6.1×10^{14}	1.5×10^{-6}	2.4×10^{-6}
K	3.0×10^{13}	7.1×10^{-8}	1.2×10^{-7}

TABLE 6. INTERSTELLAR LINES IN ζ PERSEI
IN THE RANGE $\lambda\lambda 3650 - 4350$

Rest Wavelength (\AA)	Atom or Molecule	W (m \AA)	V* (km sec $^{-1}$)
3719.935	Fe I	1.7	12.8
3859.913	Fe I	1.7	13.4
3873.369	CN R(2)	< 0.31 [†]	
3873.998	CN R(1)	3.2	13.0
3874.608	CN R(0)	11.3	12.8
3875.763	CN P(1)	1.3	12.6
3878.768	CH	1.6	13.5
3886.410	CH	4.9	13.4
3890.213	CH	3.2	13.7
3933.664	Ca II	{ 2.2	-5.8
		{ 54.5	12.4
		{ 5.5	20.7
3944.01	Al I	< 0.8 [†]	
3957.700	CH [†]	2.5	12.9
3968.470	Ca II	{ 2.6	-5.3
		{ 35.5	12.8
		{ 3.4	21.0
4226.728	Ca I	0.8	12.8
4229.337	CH [†] R(1)	< 0.56 [†]	
4232.535	CH [†] R(0)	2.8	12.3
4300.321	CH R ₂ (1)	15.5	12.5
4303.947	CH R ₁ (1)	< 0.48	

* Heliocentric velocity of line centroid.

† 99 percent confidence level upper limits.

TABLE 7. ATOMIC COLUMN DENSITIES IN THE
 $+ 13 \text{ KM SEC}^{-1}$ CLOUD IN ζ PER

Atom	λ (Å)	$N (\text{cm}^{-2}) \times 10^{-11}$
Na I	3302.34	540*
	3302.94	
Ca I	4226.728	0.03
Ca II	3933.664	9.6†
	3968.470	
Fe I	3719.935	3.4
	3859.913	5.5
Al I	3944.018	<0.5

*Determined by doublet ratio method, $b = 0.7 \text{ km sec}^{-1}$.

†Determined by doublet ratio method, $b = 2.1 \text{ km sec}^{-1}$.

TABLE 8. MOLECULAR COLUMN DENSITIES IN
THE + 13 KM SEC⁻¹ CLOUD IN ρ PER

Molecule	λ (Å)	N (cm ⁻²) × 10 ⁻¹³ *
C H	4300.321	1.5
	3890.213	2.0
	3886.410	2.0
	3878.768	1.9
C N	3874.608	0.15
	3873.998	0.10
	3875.768	0.05

* Calculated for b + 1.98 km sec⁻¹.

TABLE 9. ATOMIC PHOTOIONIZATION RATES IN THE
 ζ PER + 13 KM SEC⁻¹ CLOUD

Atom	Γ ($\times 10^{11}$) sec ⁻¹	
	high field	low field
Na I	2.7	0.88
Al I	73.	23.
Ca I	27.	8.5
Fe I	27.	9.3

TABLE 10. TOTAL ATOMIC COLUMN DENSITIES IN THE
 C PER + 13 KM SEC⁻¹ CLOUD

Atom	N (cm ⁻²)
Na	1.8×10^{15}
Ca	9.6×10^{11}
Fe	$1.3 \times 10^{14*}$
Al	$< 3.2 \times 10^{13}$

* From a weighted mean of the two Fe lines..

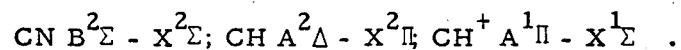
TABLE 11. A COMPARISON OF THE ATOMIC ABUNDANCES RELATIVE TO SODIUM OBSERVED AGAINST ζ OPH AND ζ PER

Atom	Fractional Abundance		
	ζ Oph	ζ Per	Solar System (Cameron 1968)
Na	1.0	1.0	1.0
Ca	0.00079	0.00053	1.2
Fe	0.070	0.72	14.1
Al	<0.018	<0.018	1.3

TABLE 12. MOLECULAR EQUIVALENT WIDTHS AND OPTICAL DEPTHS IN THE ζ OPH - 15 KM SEC⁻¹ CLOUD

Molecule	Line *	$\lambda_{\text{air}}(\text{\AA})$	$W(\text{m\AA})^\dagger$	τ^\S
CN	R(0)	3874.608	8.27 ± 0.10	0.338 ± 0.003
	R(1)	3873.998	2.78 ± 0.10	0.105 ± 0.004
	P(1)	3875.763	1.40 ± 0.10	0.052 ± 0.004
	R(2)	3873.369	<0.17	<0.0062
CH	R ₂ (1)	4300.321	19.6	0.719
	R ₁ (1)	4303.947	<0.28	<0.0081
CH [†]	R(0)	4232.535	24.1	0.968
	R(1)	4229.337	<0.22	<0.0065

* Of the (0, 0) bands of the following electronic systems:



† Upper limits represent a confidence level of 99 percent; uncertainty on measurements is one standard deviation.

§ Computed from the curve of growth for gaussian lines, using

$$b = 1.36 \text{ km sec}^{-1}.$$

TABLE 13. TEMPERATURE OF THE BACKGROUND RADIATION
AT $\lambda 2.64$ MM, FROM INTERSTELLAR CN IN ζ OPH

	Line Ratio	
	R(1)/R(0)	P(1)/R(0)
T_{10} (CN), uncorrected ($^{\circ}$ K) ^a	2.99 ± 0.07	2.99 ± 0.17
Correction for curve of growth ($^{\circ}$ K) ^b	-0.07	-0.09
Correction for electrons and H I ($^{\circ}$ K)	-0.17 ± 0.10	-0.17 ± 0.10
T_B (2.64mm) ($^{\circ}$ K)	2.75 ± 0.12	2.73 ± 0.20
T_B (2.64mm), weighted mean ($^{\circ}$ K) ^d	2.75 ± 0.10	

^aOptical depths derived from equivalent widths in Table 12, assuming $b = 2.40 \text{ km sec}^{-1}$ as measured from the unsmoothed spectrum in Figure 4.

^bAdopting $b(\text{CN}) = 1.36 \text{ km sec}^{-1}$.

^cTaking $n_e = 0.36 \pm 0.19 \text{ cm}^{-3}$ and $n(\text{HI}) = 350 \pm 350 \text{ cm}^{-3}$.

^dRelative weights 4:1. The quoted uncertainty is one standard deviation. This includes no contribution for uncertainty in the curve of growth correction, which is felt to be at most comparable to the other uncertainties.

TABLE 14. UPPER LIMITS ON BACKGROUND RADIATION FROM
INTERSTELLAR MOLECULAR LINES IN ζ OPH

Molecule	Line Ratio	Wavelength (mm)	Upper Limit on T_B ($^{\circ}$ K)	Upper Limit on $I_{\nu} \times 10^{14}$ (erg cm $^{-2}$ sec $^{-1}$ ster $^{-1}$ Hz $^{-1}$)
CN	R(2)/R(1)	1.32	3.37	0.72
CH	R ₁ (1)/R ₂ (1)	0.559	5.23	1.66
CH ⁺	R(1)/R(0)	0.359	7.37	3.75

TABLE 15. STARS OBSERVED

Name	MK Type	V	E_{B-V}	$\alpha(1900)$ (hr)	$\delta(1900)$ (o)	Number of Plates	Dispersion (\AA mm^{-1})	CN
ζ Per	B1Ib	2.83	0.13	3 47 51	+31 35	6	1.3	yes
X Per	Ope	6.08	0.31	3 49 8	+30 45	1	1.3	yes
ζ Oph	O9.5 V	2.56	0.28	16 31 39	-10 22	31	1.3	yes
HR6825	A0Ia	6.08	-	18 9 38	-18 42	1	2.6	no
20 Aql	B3IV	5.37	-	19 7 15	- 8 6	1	1.3	yes
HR7573	A1Iab	5.58	0.70	19 47 49	+24 44	1	2.6	yes
HR7835	A1Ib	5.88	0.47	20 25 32	+36 7	1	2.6	no
HR8334	A2Ia	4.28	0.49	21 42 34	+60 40	1	2.6	no
13 Cep	B8Ib	5.79	0.76	21 51 31	+56 8	1	2.6	yes
HR8541	B9Iab	4.53	0.09	22 20 28	+48 58	1	2.6	no
HR9100	A0III	5.89	0.27	23 59 4	+61 44	1	2.6	no

TABLE 16. CN EQUIVALENT WIDTHS AND OPTICAL DEPTHS

Star	Line	W(mÅ)*	τ^\dagger
ζ Per	R(0)	11.3 ± 0.19	0.274 ± 0.005
	R(1)	3.2 ± 0.19	0.072 ± 0.005
X Per	R(0)	14.7 ± 1.5	0.45 ± 0.05
	R(1)	6.9 ± 1.5	0.19 ± 0.05
ζ Oph	R(0)	8.27 ± 0.10	0.338 ± 0.003
	R(1)	1.40 ± 0.10	0.105 ± 0.004
20 Aql	R(0)	9.3 ± 0.9	0.27 ± 0.03
	R(1)	3.5 ± 0.9	0.095 ± 0.025
HR7573	R(0)	5.0	0.14
	R(1)	< 1.9	<0.05
13 Ceph	R(0)	19.3 ± 1.7	0.62 ± 0.07
	R(1)	7.4 ± 1.7	0.21 ± 0.05

*Uncertainty on measurements is one standard deviation; upper limit represents a confidence level of 99 percent.

† Computed with $b = 1.98 \text{ km sec}^{-1}$ for ζ Per, 1.36 km sec^{-1} for ζ Oph, and 1.67 km sec^{-1} for all other stars.

TABLE 17. CN EXCITATION TEMPERATURES

Star	V	MK Type	$\Pi_{b_0}^{\Pi}$	$\Pi_{I_0}^{\Pi}$	$T_{10}(\text{CN})$ ($^{\circ}\text{K}$)	Radial Velocity (km sec^{-1})	
						CN	H I*
ζ Oph	2.56	O9.5V	+23.6	6.3	2.75 ± 0.10 §	15.2	-12.8
ζ Per	2.83	B1Ib	-16.7	162.3	2.66 ± 0.12 §	12.8	13.4
AE Aur*	5.3	O8.5V	-2.3	172.1	3.5 ± 2.3		
20 Aql	5.37	B3IV	-8.3	28.2	3.1 ± 0.7	-13.8	-2.0, -11.5
HR618 ⁺	5.68	A1Ia	-3.0	132.9	3.7 ± 0.7		
13 Ceph	5.79	B8Ib	+1.7	100.4	3.1 ± 0.6	-3.3	
X Per	6.08	O pe	-17.1	163.1	3.5 ± 0.8	15.6	13.0
BD + 66 ^o 1675*	9.05	O7	+4.8	118.0	2.4 ± 0.6	-17.4	-14.2, -19.5
BD + 66 ^o 1674*	9.5	O	+4.8	118.0	2.5 ± 0.6	-17.4	-14.2, -19.5

* Clauser and Thaddeus (1969)

+ Peimbert (1968)

§ Corrected for collision with electrons and neutral atoms

REFERENCES

- Adams, W. S. 1941, Ap. J., 93, 11.
_____, 1949, Ap. J., 109, 354.
- Allison, A. C., and Dalgarno, A. 1971, Astron. and Astrophys.,
13, 331.
- Alpher, R. A., Bethe, H., and Gamow, G. 1948, Phys. Rev.,
73, 803.
- Alpher, R. A., and Herman, R. C. 1949, Phys. Rev. 75, 1089.
_____, 1951, Phys. Rev., 84, 60.
- Augason, G. C., and Herbig, G. H. 1967, Ap. J., 150, 729.
- Beals, C. S., and Oke, J. B. 1953, M. N., 113, 530.
- Bennett, R. G., and Dalby, F. W. 1962, J. Chem Phys., 36, 399.
- Blair, A. G., Beery, J. G., Edeskuty, F., Hiebert, R. D.,
Shipley, J. P., and Williamson, K. D., Jr. 1971, Phys.
Rev. Letters, 27, 1154.
- Bless, R. C., and Savage, B. D. 1970, in Ultraviolet Stellar Spectra
and Related Ground Based Observations (I. A. U. Symp. No. 36),
ed. L. Houziaux and H. E. Butler (Dordrecht: Reidel)
- Borgman, J., and Blaauw, A. 1963, B. A. N., 17, 358.
- Bortolot, V. J., Jr., Clauser, J. F., and Thaddeus, P. 1969,
Phys. Rev. Letters, 22, 307.
- Bortolot, V. J., Jr., and Thaddeus, P. 1969, Ap. J. (Letters), 155, L17.
- Burgess, A., Field, G. B., and Michie, R. W. 1960, Ap. J., 131, 529.

- Cameron, A. G. W. 1968, in Origin and Distribution of the Elements,
ed. L. H. Ahrens (Oxford: Pergamon).
- Carruthers, G. R. 1970, Ap. J. (Letters), 161, L81.
- Clauser, J. F. 1970, unpublished Ph. D. dissertation, Dept. of
Physics, Columbia.
- Clauser, J. F., and Thaddeus, P. 1972, Proc. 3rd International
Conf. on Relativistic Astrophysics, (to be published).
- Corliss, C. H., and Bozman, W. R. 1962, Experimental Transition
Probabilities for Spectral Lines of Seventy Elements;
NBS Monograph 53.
- Davenport, W. B., and Root, W. L. 1958, An Introduction to the
Theory of Random Signals and Noise (New York: McGraw Hill).
- de Vaucouleurs, G. 1968, Applied Optics, 7, 1513.
- Dicke, R. H., Peebles, P. J. E., Roll, P. G., and Wilkinson, D. T.
1965, Ap. J., 142, 414.
- Ditchburn, R. W., and Hudson, R. D. 1960, Proc. Roy. Soc.
London (A), 256, 53.
- Douglas, A. E., and Herzberg, G. 1942, Can. J. Res., 20A, 71.
- Field, G. B., Goldsmith, D. W., and Habing, H. J. 1969, Ap. J.
(Letters), 155, L149.
- Field, G. B., and Hitchcock, J. L. 1966, Phys. Rev. Letters, 16, 817.
- Fink, E. H., and Welge, K. H. 1967, J. Chem. Phys., 46, 4315.
- Fowler, W. A., Caughlan, G. R., and Zimmerman, B. A.
1967, Ann. Rev. Astr. and Astrophys., 5, 525.

- Frisch, P. 1972, Ap. J., 173, 301.
- Gamow, G. 1948, Phys. Rev., 74, 505.
- Gerö, L. 1941, Z. Physik, 118, 27.
- Goldsmith, D. W., Habing, H. J., and Field, G. B. 1969, Ap. J.,
158, 173.
- Habing, H. J. 1968, B. A. N., 19, 421.
_____. 1969, B. A. N., 20, 177.
- Hegyí, D., Traub, W., and Carleton, N. 1972 (to be published).
- Helstrom, C. W. 1968, Statistical Theory of Signal Detection
(New York: Pergamon).
- Herbig, G. H. 1968, Z. für Astrophysik, 68, 243.
- Herzberg, G. 1959, The Spectra of Diatomic Molecules
(New York: McGraw-Hill).
- Hickock, F. R., and Morton, D. C. 1968, Ap. J., 152, 203.
- Hjellming, R. M., Gordon, C. P., and Gordon, K. J. 1969,
Astron. and Astrophys., 2, 202.
- Hobbs, L. M. 1965, Ap. J., 142, 160.
_____. 1969, Ap. J., 157, 135.
- Hobbs, L. M., and Zuckerman, B. 1972, Ap. J., 171, 17.
- Houck, J. R., and Harwit, M. O. 1969, Ap. J. (Letters),
157, L45.
- Howard, W. E., Wentzel, D. G., and McGee, R. X. 1963,
Ap. J., 138, 988.

- Hudson, R. D., and Carter, V. L. 1965, Phys. Rev., 139, A1426.
_____. 1967a, Ap. J., 149, 229.
_____. 1967b, J. Opt. Soc. Am., 57, 651.
- Jefferts, K. B., Penzias, A. A., and Wilson, R. W. 1970,
Ap. J. (Letters), 161, L87.
- Jenkins, F. A., and Wooldridge, D. E. 1938, Phys. Rev., 53, 137.
Ap. J. (Letters), 161, L87.
- Kelly, H., and Ron, A. 1971, Phys. Rev. Letters, 26, 1359.
- Kozlov, M. G., Nikonova, E. I., and Startsev, G. P. 1966,
Optics and Spectr., 21, 298 (USSR).
- Latham, D. W. 1969, Bull. A. A. S., 1, 147.
- Lillie, C. F. 1968, unpublished Ph.D. dissertation,
Dept. of Astronomy, Univ. of Wisc.
- Lynds, B. 1969, P. A. S. P., 81, 496.
- Mather, J. C., Werner, M. W., and Richards, P. L. 1971,
Ap. J. (Letters), 170, L59.
- McKellar, A. 1951, Publ. Dominion Astrophys. Observatory,
Victoria, B. C., 7, 251.
_____. 1965, in Stellar Atmospheres, ed. J. L. Greenstein,
(Chicago: Univ. of Chicago).
- Merrill, P. W., Sanford, R. F., Wilson, O. C., and Burwell, C. G.
1937, Ap. J., 86, 274.

Moore, C. E. 1945, A Multiplet Table of Astrophysical Interest

(Princeton: Princeton Observatory).

Muehlner, D., and Weiss, R. 1970, Phys. Rev. Letters, 24, 742.

_____. 1972 (to be published).

Münch, G. 1957, Ap. J., 125, 42.

_____. 1964, *ibid.*, 140, 107.

Newsom, G. H. 1966, Proc. Phys. Soc., 87, 975.

Osterbrock, D. E. 1964, Ann. Rev. Astr. and Astrophys., 2, 95.

Peimbert, M. 1968, Bull. Obs. Tonantzintla y Tacubaya, 4, 233.

Penzias, A. A., Jefferts, K. B., and Wilson, R. W. 1972,

Phys. Rev. Letters, 28, 772.

Penzias, A. A., and Wilson, R. W. 1965, Ap. J., 142, 419.

Pipher, J. L., Houck, J. R., Jones, B. W., and Harwit, M. O.

1971, Nature, 231, 375.

Rees, M. J., Sciama, D. W., and Stobbs, S. H. 1968, Ap. Letters,

2, 243.

Rogers, A. E. E., and Barrett, A. H. 1966, A. J., 71, 868.

Rogerson, J. B., Spitzer, L., Jr., and Bahng, J. D. 1959,

Ap. J., 130, 991.

Seaton, M. J. 1951, M. N., 111, 368.

_____. 1959, *ibid.*, 119, 81.

Scherb, F. 1968, Ap. J. (Letters), 153, L55.

- Shane, C. D., and Wirtanen, C. A. 1967, Publ. Lick Obs.,
22, Pt. 1.
- Shivanandan, K., Houck, J. R., and Harwit, M. O. 1968,
Phys. Rev. Letters, 21, 1460.
- Silk, J., and Werner, M. W. 1969, Ap. J., 158, 185.
- Smith, A. M. 1972 (to be published).
- Smith, A. M., and Stecher, T. P. 1971, Ap. J. (Letters), 164, L43.
- Spitzer, L., Jr. 1948, Ap. J., 108, 276.
_____. 1968, Diffuse Matter in Space (New York: Wiley).
- Spitzer, L., Jr. and Tomasko, M. G. 1968, Ap. J., 152, 971.
- Stecher, T. P. 1968, Bull. Astr. Inst. Czech., 19, 279.
- Strömgren, B. 1948, Ap. J., 108, 242.
- Thaddeus, P. 1972, Ann. Rev. Astr. and Astrophys., (to be published).
- Thaddeus, P., and Clauser, J. F. 1966, Phys. Rev. Letters,
16, 819.
- Van Citters, G. W., and Morton, D. C. 1970, Ap. J., 161, 695.
- Whitford, A. E. 1958, A. J., 63, 201.
- White, R. E. 1972 (to be published).
- Wiese, W. L., Smith, M. W., and Miles, B. M. 1969, Atomic
Transition Probabilities, Volume II: Sodium through Calcium,
NSRDS-NBS 22.
- Wilson, O. C. 1948, P. A. S. P., 60, 198.
- Witt, A. N., and Lillie, C. F. 1971, (to be published).

Wright, K. O. 1969, Bull. A. A. S., 1, 142.

Zadeh, L. A., and Ragazzini, J. R. 1952, Proc. I. R. E.,

40, 1223.

Zimmermann, H. 1964, Astron. Nachr., 288, 99.

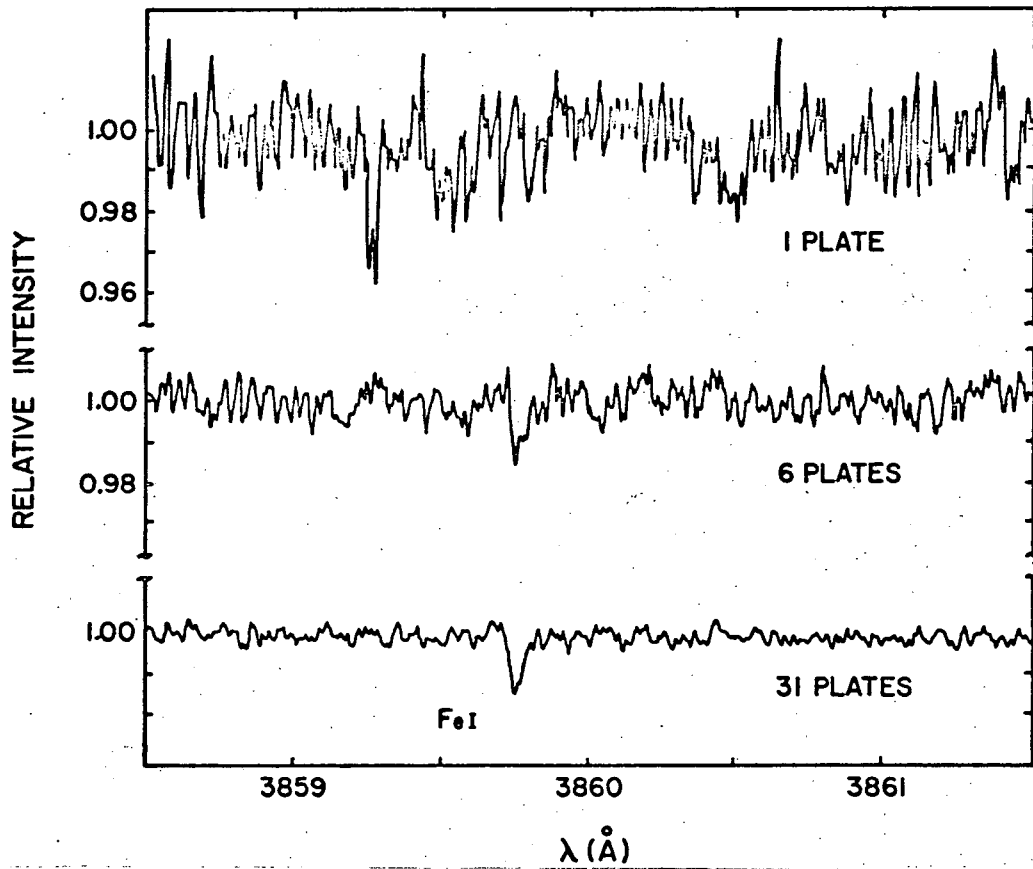


Figure 1. The increase in sensitivity due to the synthesis technique. Fe I λ 3860 Å in ζ Oph is shown for a single good plate and for two stages of synthesis.

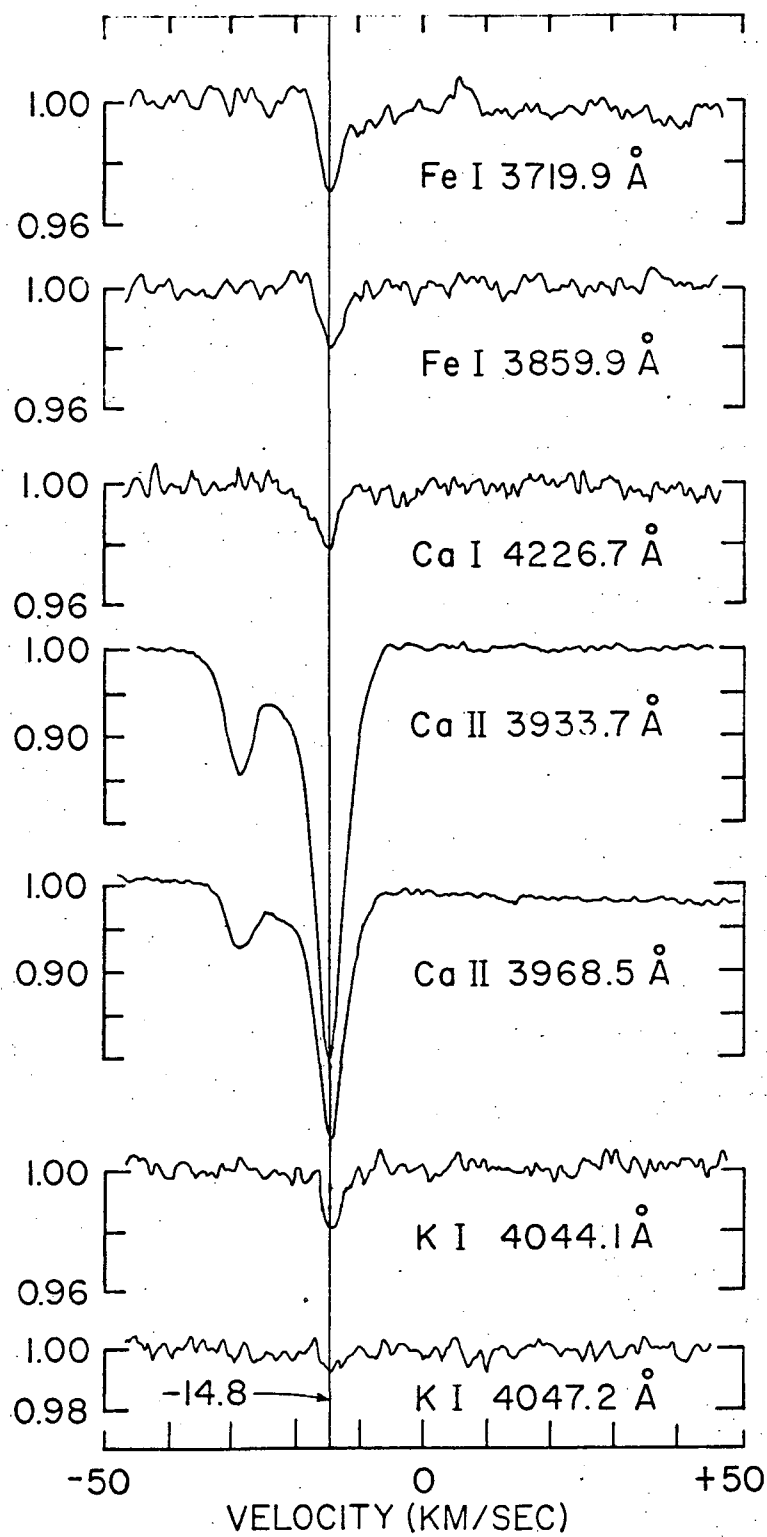


Figure 2. The atomic line profiles observed against ζ Oph in the interval $\lambda\lambda 3650-4350 \text{ \AA}$ plotted against heliocentric velocity.

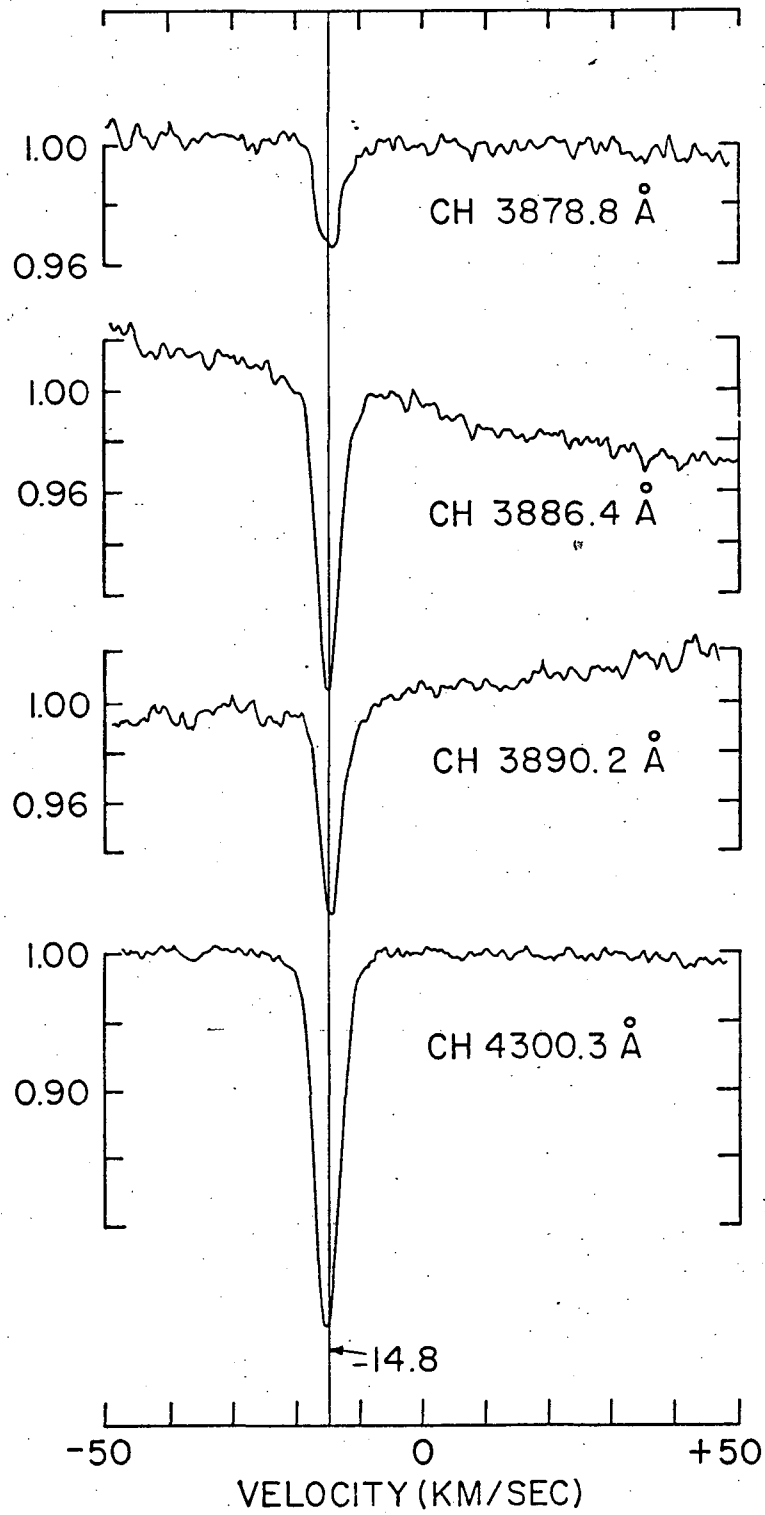


Figure 3. The molecular line profiles observed against ζ Oph in the interval $\lambda\lambda 3650\text{--}4350 \text{ \AA}$ plotted against heliocentric velocity.

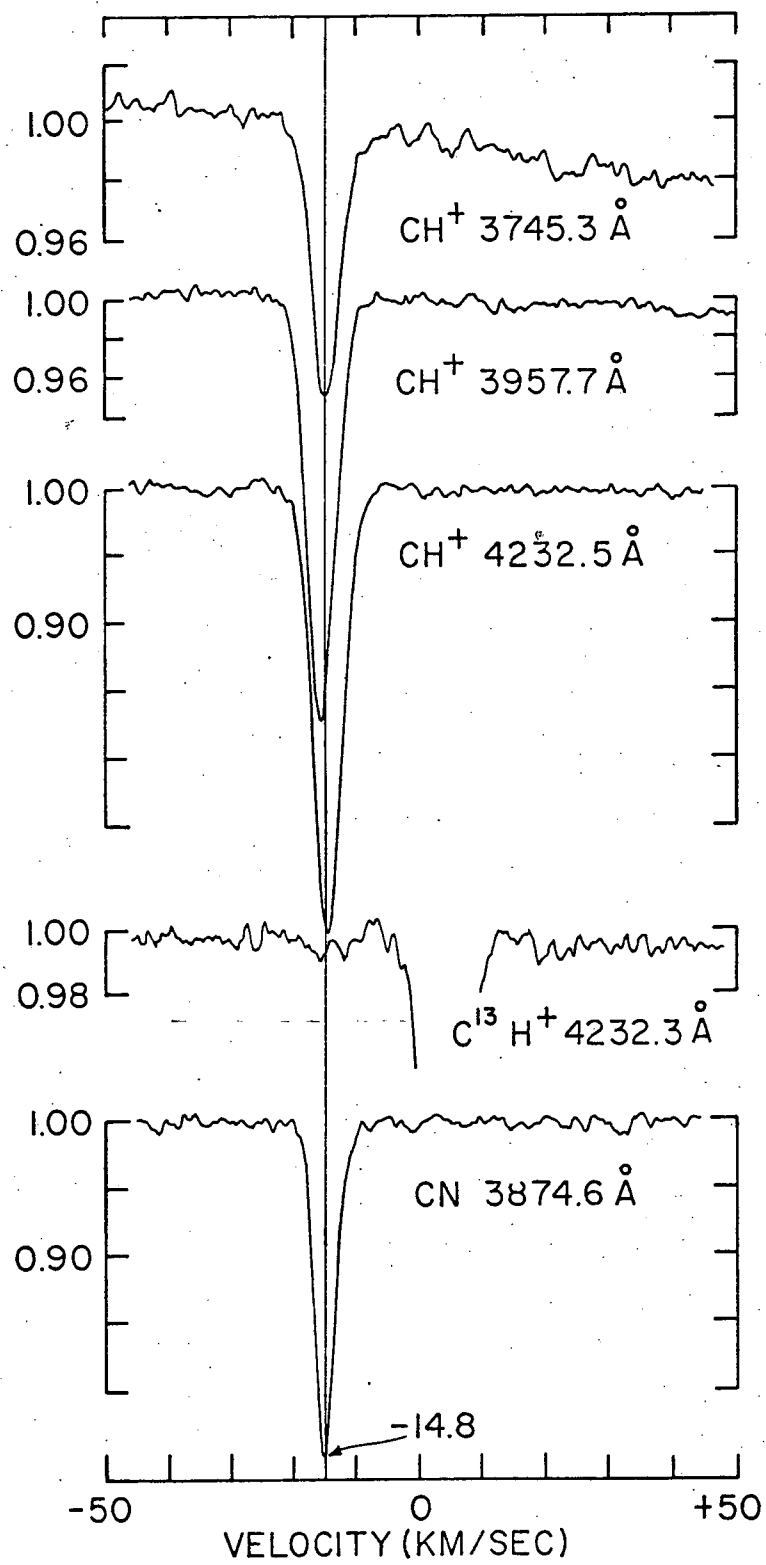


Figure 3. (cont'd)

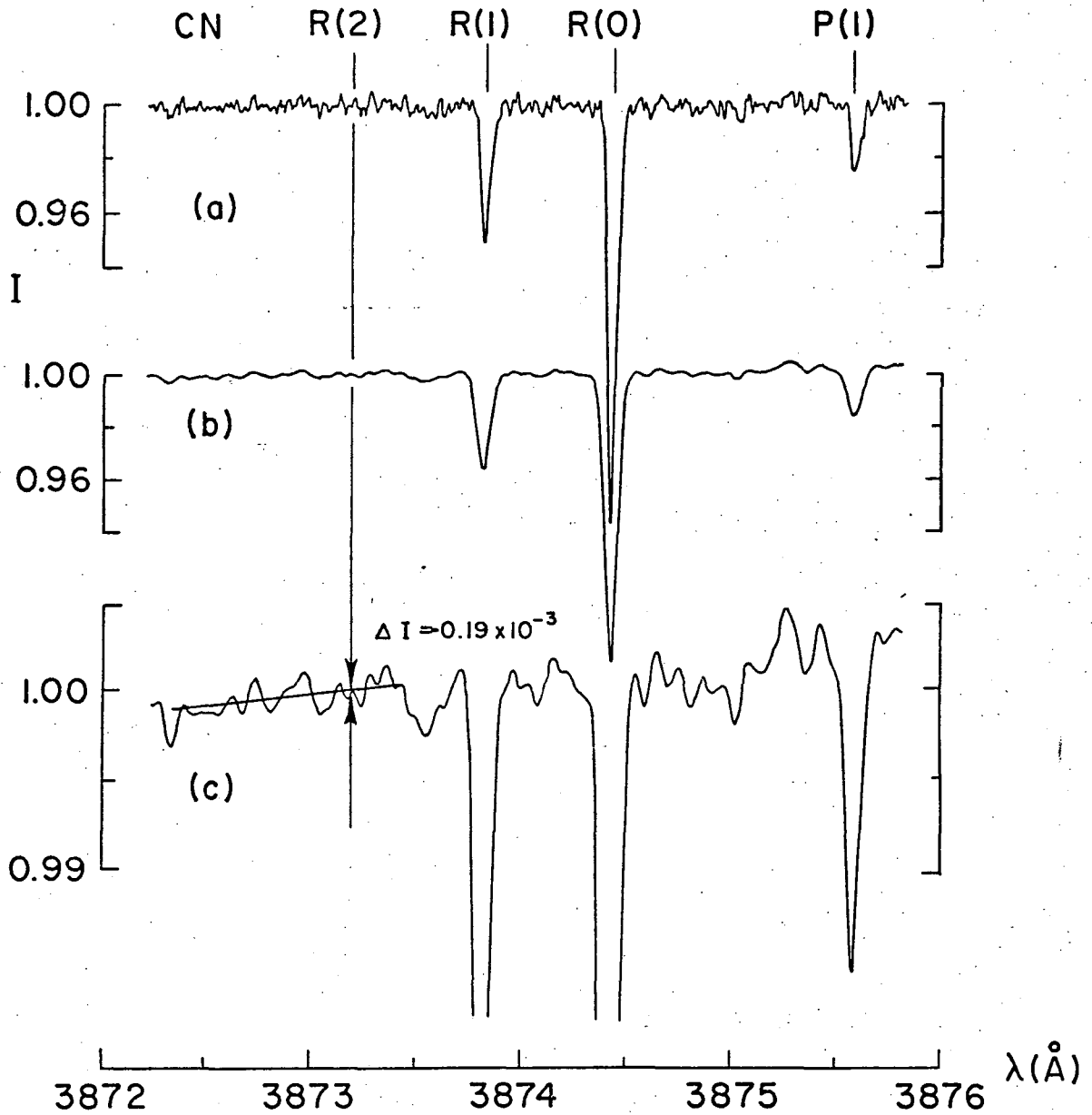


Figure 4. The $\lambda 3875 \text{ \AA}$ CN band in ζ Oph. Trace (a) is the unfiltered synthesis, (b) is filtered with a 0.050 \AA FWHM gaussian, and (c) is a magnification of (b). The vertical line marks the position of R(2) and the short line through the magnified spectrum is the best straight line continuum fit to the interval it subtends. **111**

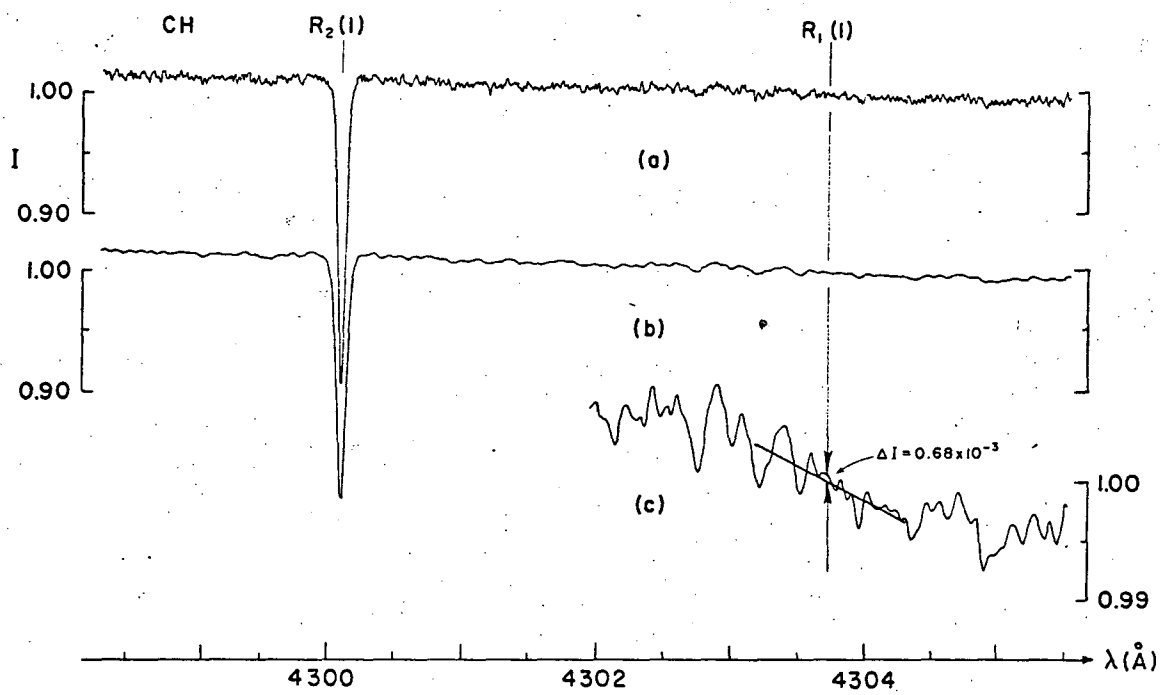


Figure 5. The $\lambda 4232 \text{\AA}$ CH band in ζ Oph.

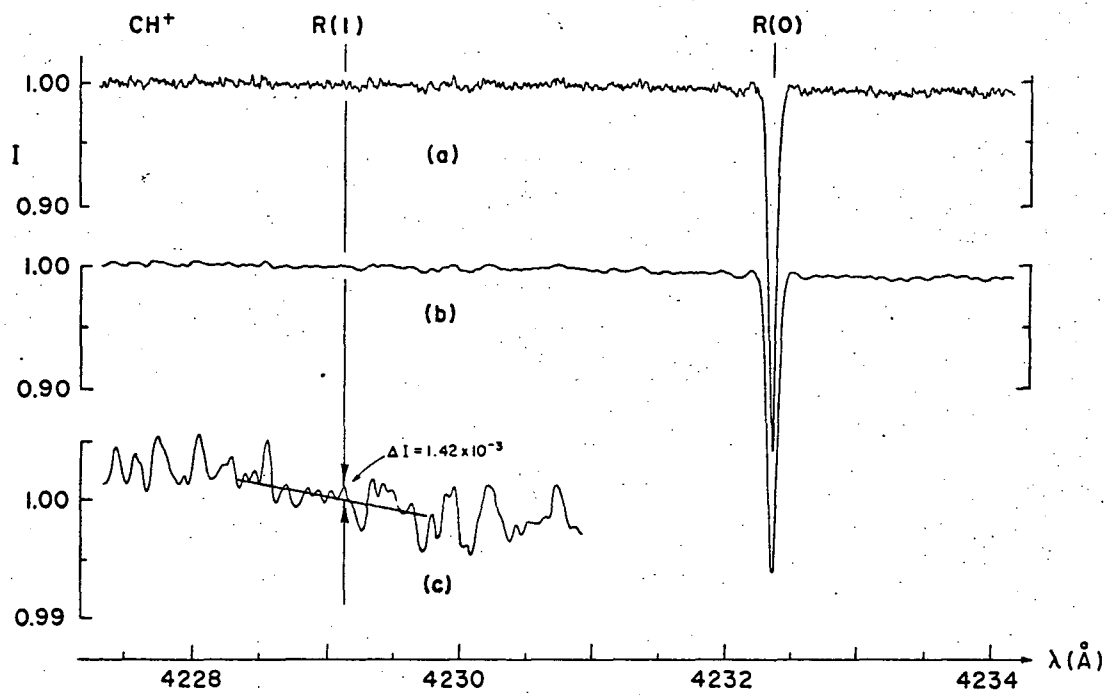


Figure 6. The $\lambda 4232 \text{ \AA}$ CH^+ band in $\zeta \text{ Oph}$.

Figure 7. The high and low radiation fields adopted at the position of the ζ Oph-15 km sec⁻¹ cloud. The high field is that of ζ Oph at a distance of 15 pc plus the galactic field of Habing (1968), both attenuated by the cloud itself. The low field is the attenuated galactic field alone.

Figure 8. The adopted photoionization cross-section of Ca I. From $\lambda\lambda$ 2028 to 1660 Å, the recommendations of Hudson and Carter (1967a) have been followed. The cross-sections of Newsom (1966) have been adopted after multiplication by 1.5, except at the peaks of the strong $\lambda\lambda$ 1886 and 1765 Å autoionizing lines, where Hudson and Carter's own values were accepted. In the range $\lambda\lambda$ 1660 to 1080 Å, 1.5 times the cross-sections of Ditchburn and Huson (1960) have been used, while below λ 1080 Å the constant value $a_{\lambda} = 1.0$ Mb has been assumed.

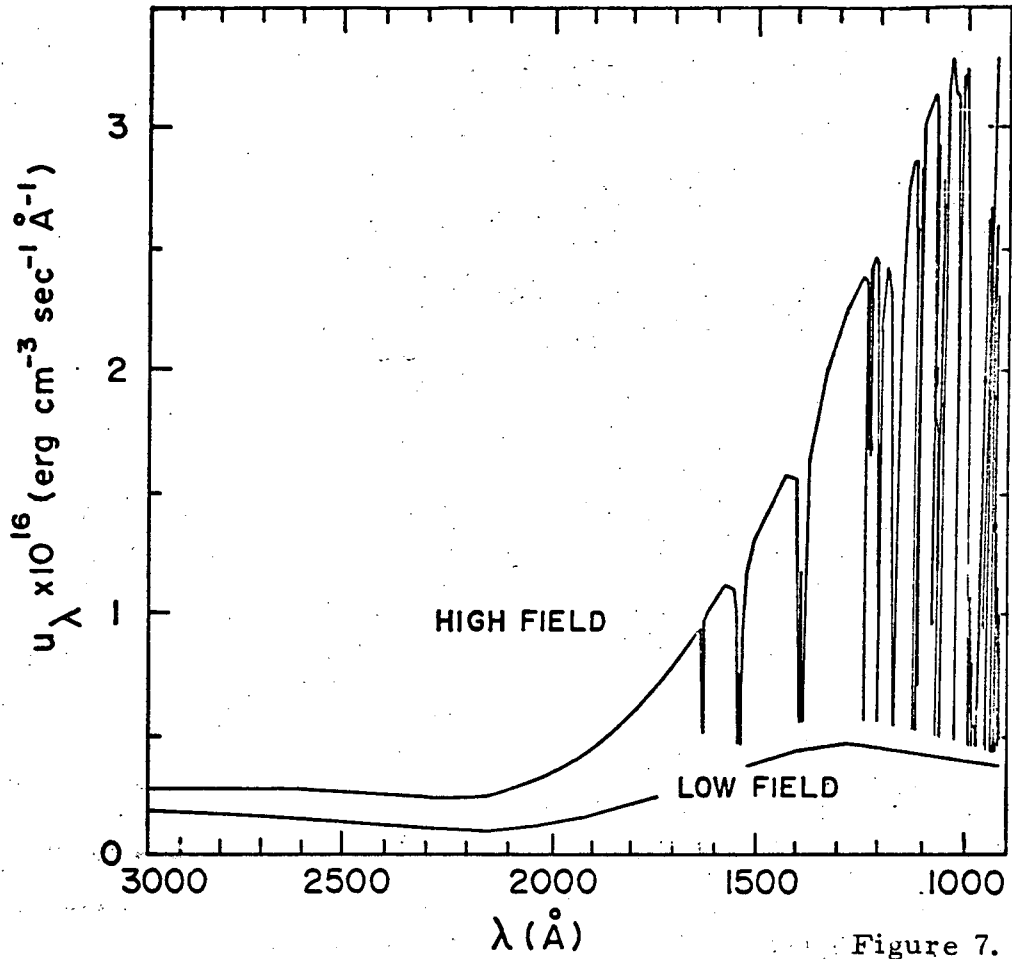


Figure 7.

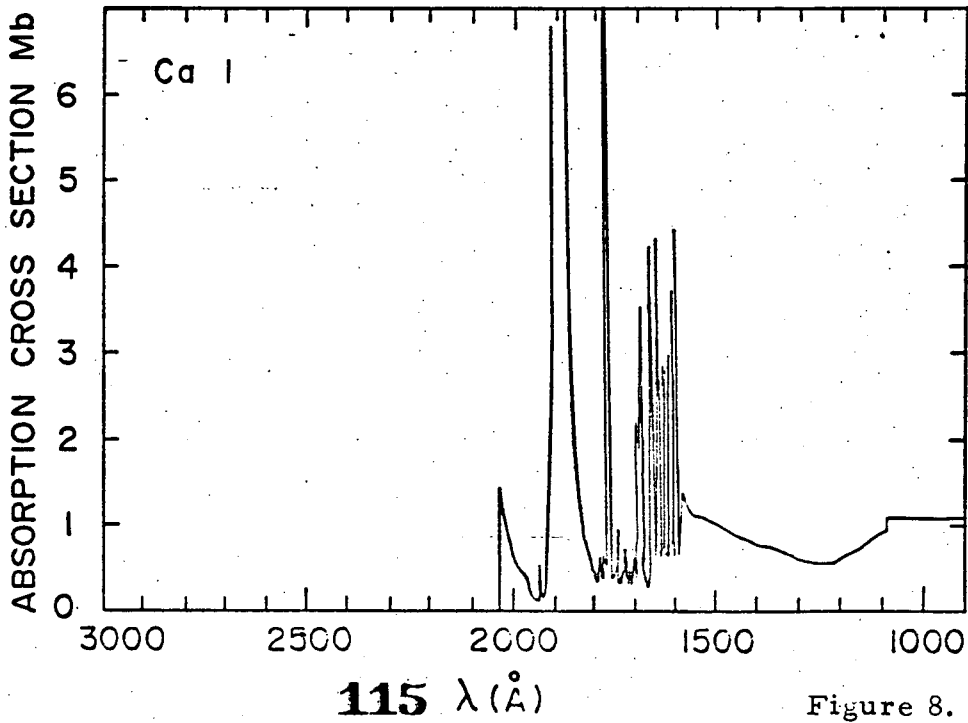


Figure 8.

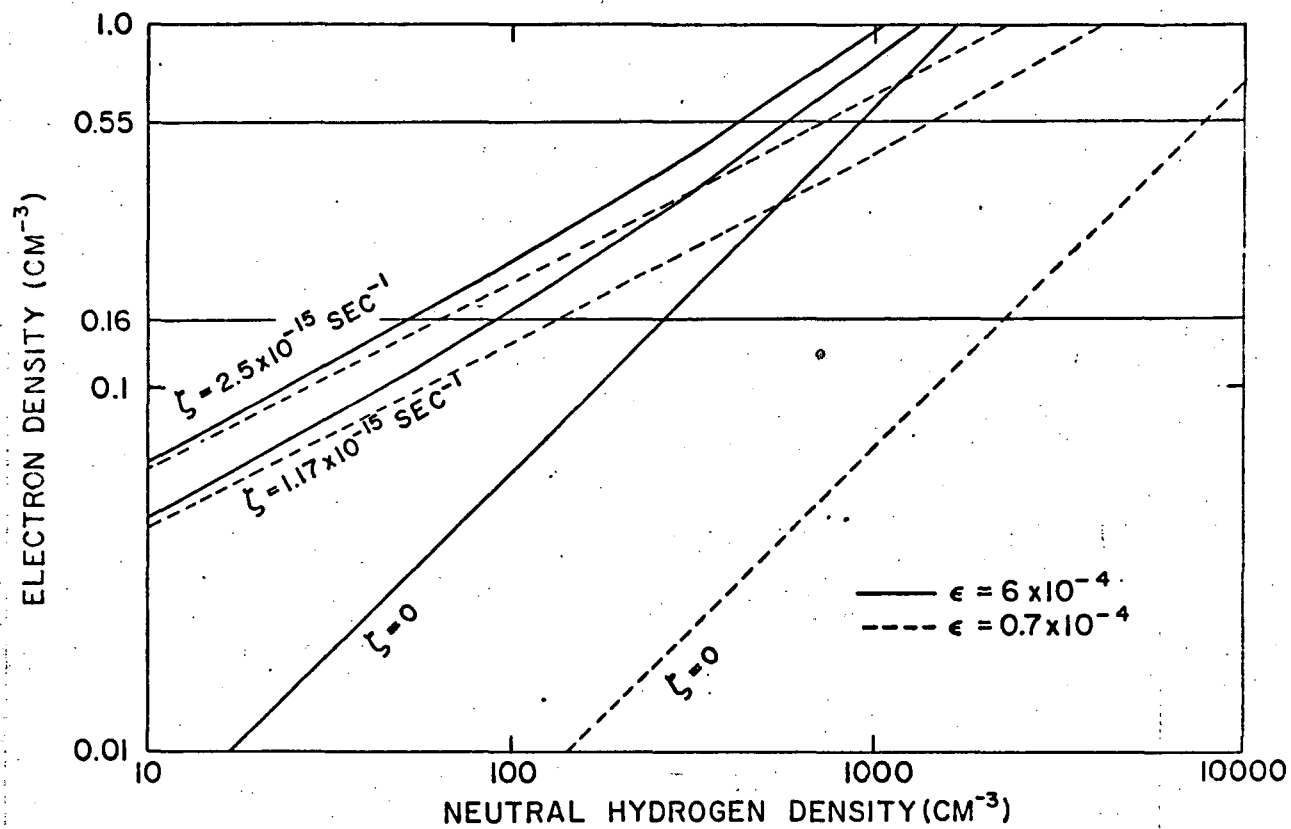


Figure 9. The electron density as a function of neutral hydrogen density and trace element abundance. The horizontal lines at $n_e = 0.16$ and 0.55 cm^{-3} represent the limits derived for the $\zeta \text{ Oph} - 15 \text{ km sec}^{-1}$ cloud.

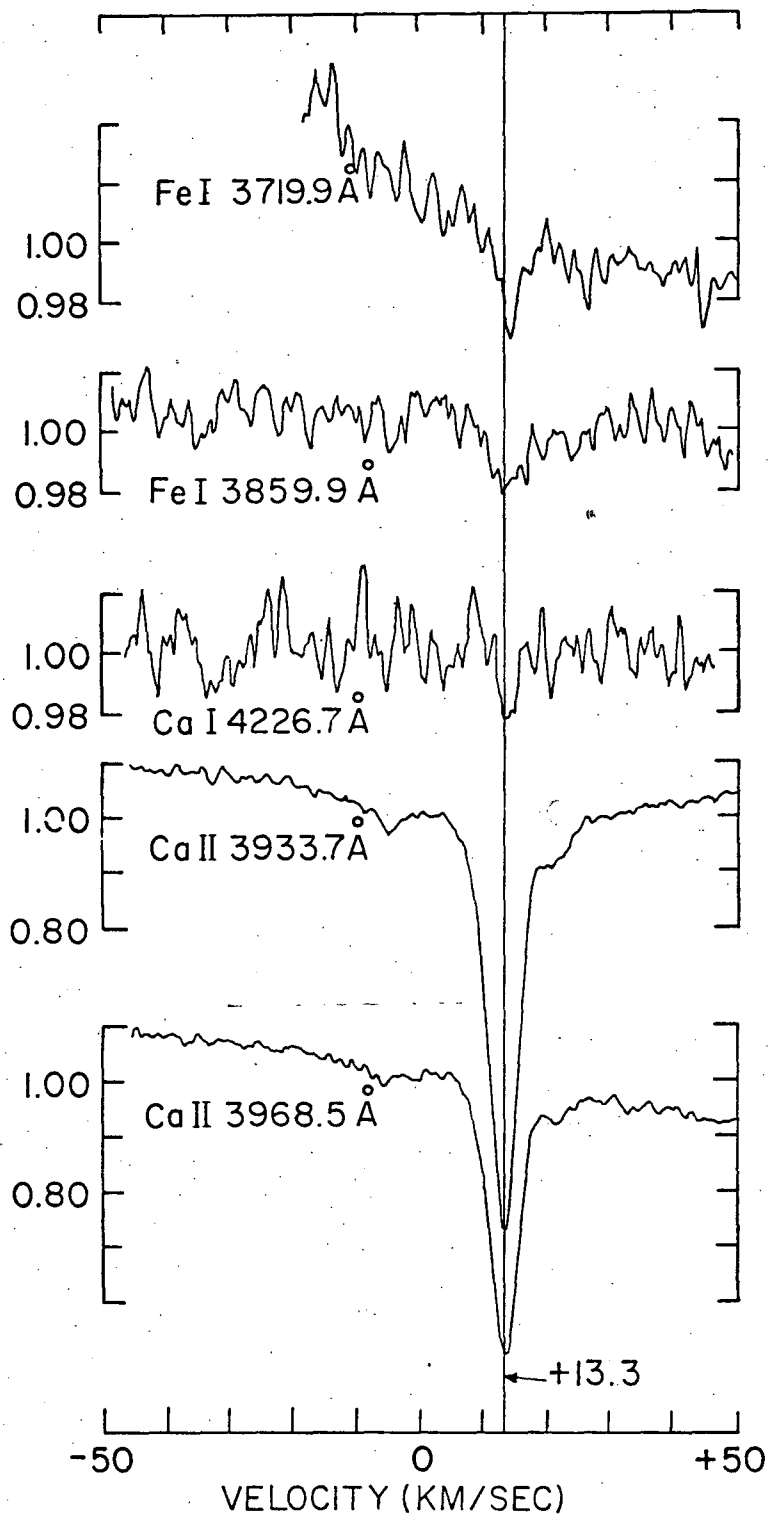


Figure 10. The atomic line profiles observed against ζ Per in the interval $\lambda\lambda$ 3650 - 4350 Å, plotted against heliocentric velocity. **117**

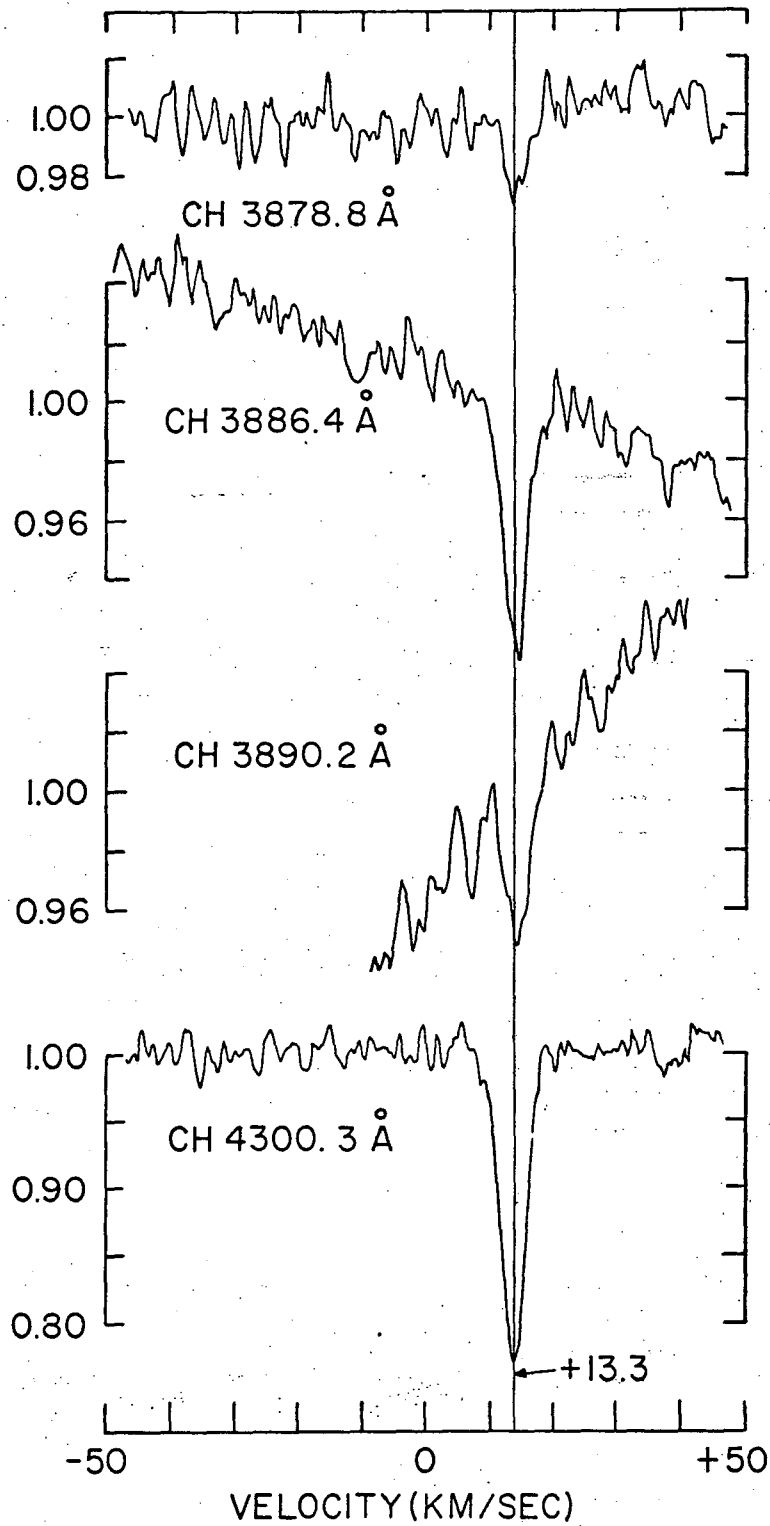


Figure 11. The molecular line profiles observed against ζ Per in the interval $\lambda\lambda 3650 - 4350 \text{ \AA}$, plotted against heliocentric velocity.

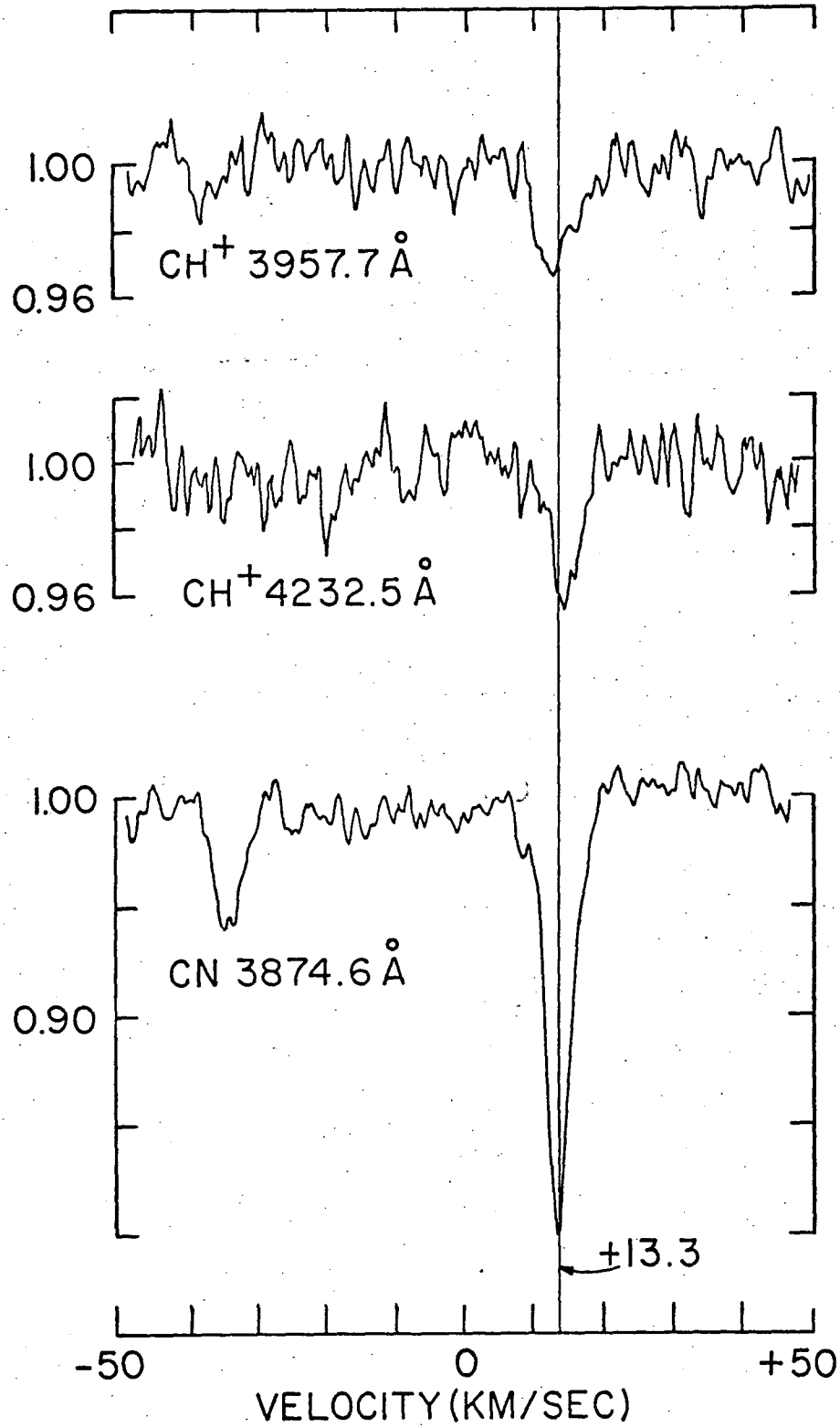


Figure 11. (cont'd)

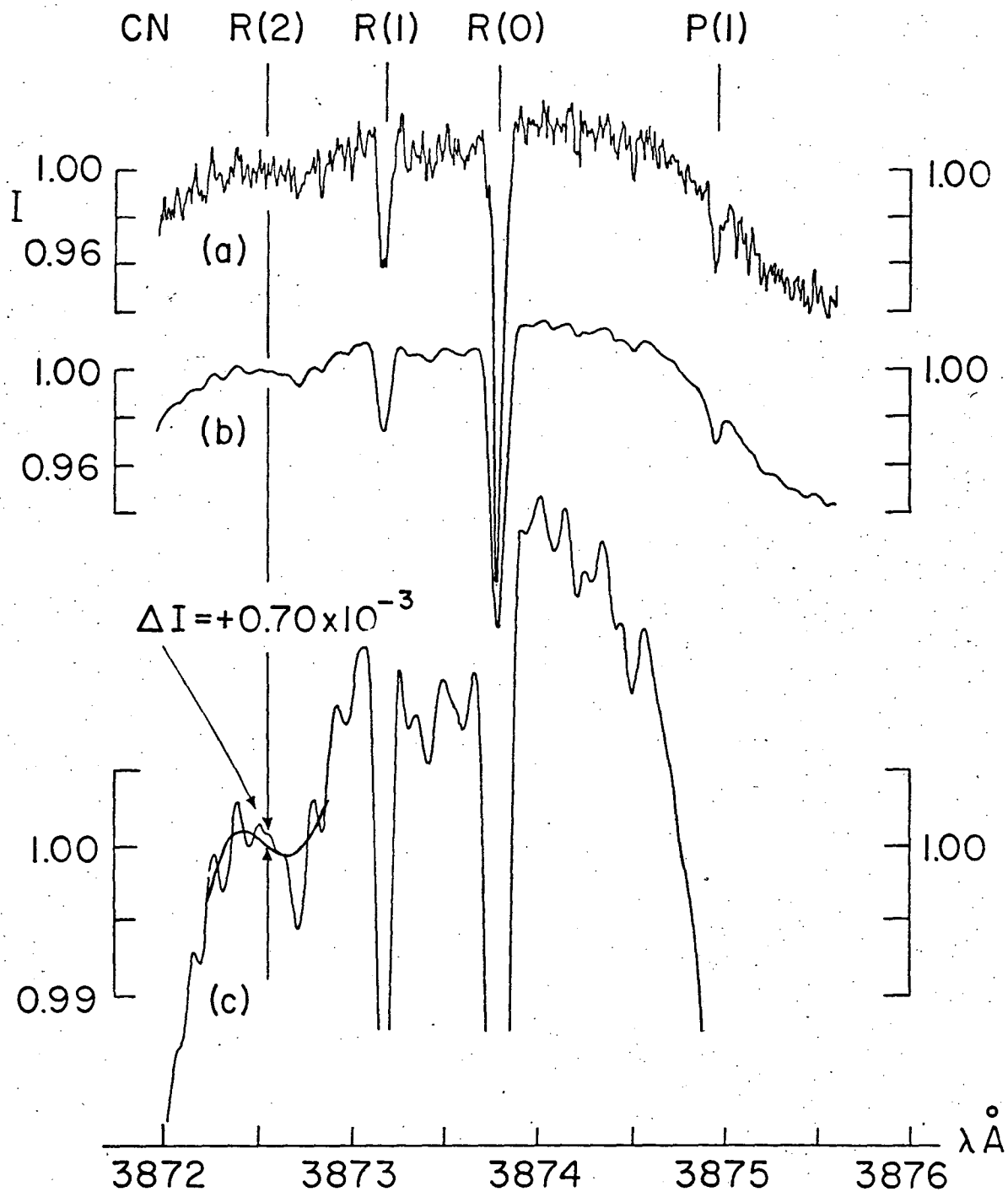


Figure 12. The vicinity of the $\lambda 3875 \text{ \AA}$ CN band in ζ Per.

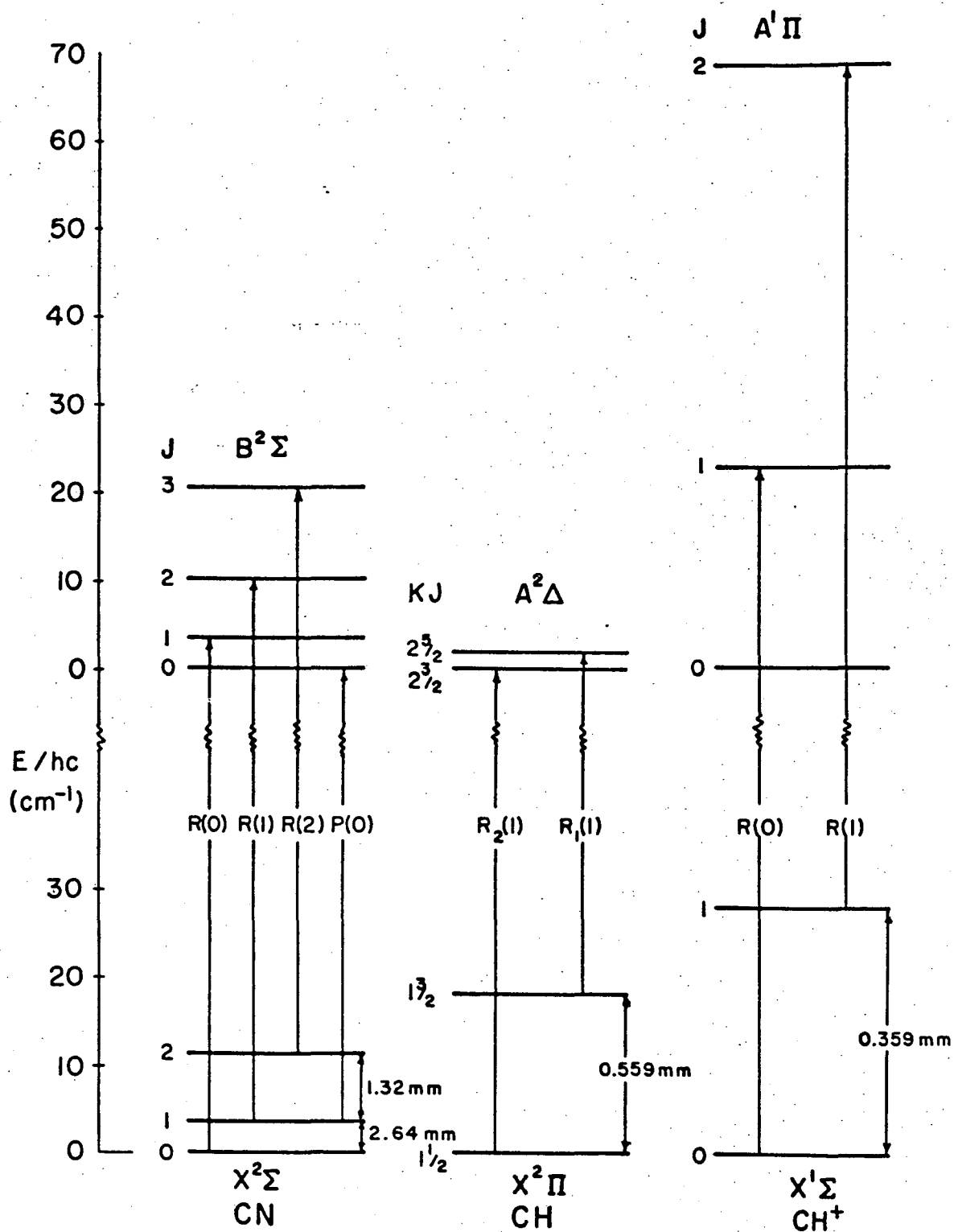


Figure 13. Partial term diagrams of CN, CH, and CH⁺, showing the transitions relevant to determination of the microwave background radiation intensity.

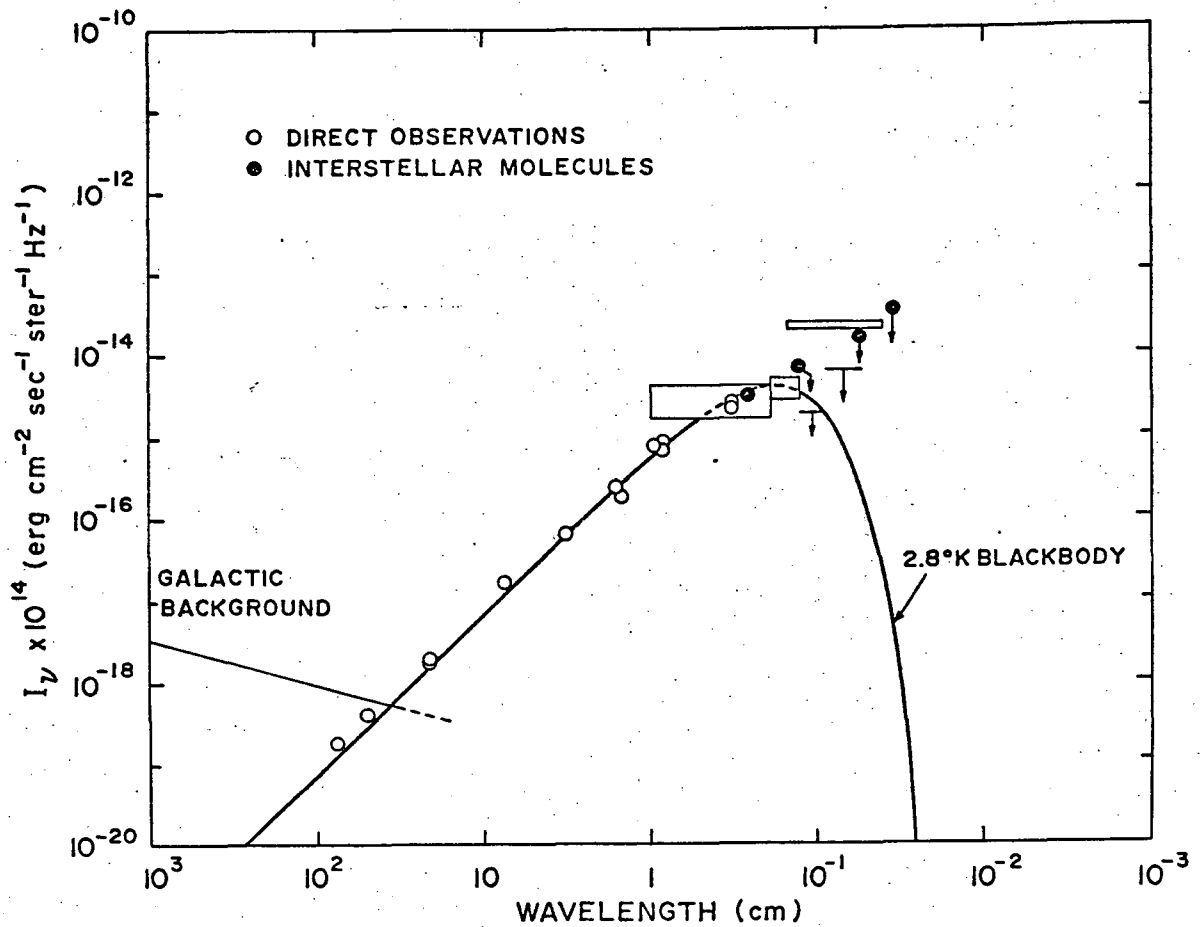


Figure 14. Direct and indirect measurements of the microwave background radiation. Open circles are the direct ground-based measurements (see Thaddeus 1972 for references), closed circles are the indirect measurements obtained from the CN, CH and CH⁺ interstellar bands in ζ Oph (Tables 13 and 14), C represents the most recent Cornell rocket results, and M the most recent MIT balloon results after correction for atmospheric emission.

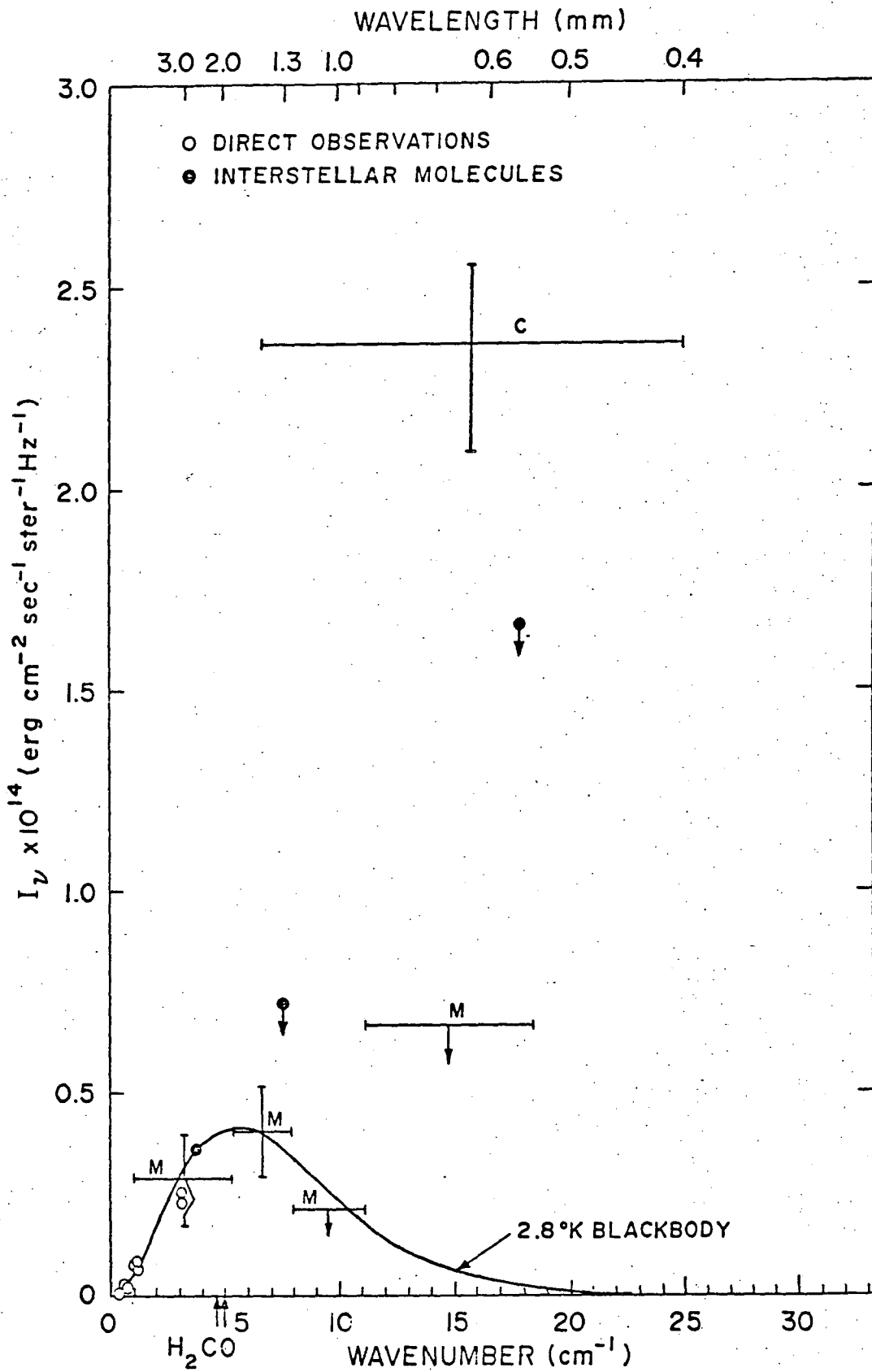


Figure 15. Figure 14 on a linear scale. The CH^+ upper limit is off scale and not shown.